

Lung epithelial cells are essential effectors of inducible resistance to pneumonia

JO Cleaver¹, D You¹, DR Michaud¹, FA Guzmán Pruneda^{1,2}, MM Leiva Juárez², J Zhang³, PM Weill¹, R Adachi^{1,4}, L Gong¹, SJ Moghaddam^{1,4}, ME Poynter⁵, MJ Tuvim^{1,4} and SE Evans^{1,4,6}

Infectious pneumonias are the leading cause of death worldwide, particularly among immunocompromised patients. Therapeutic stimulation of the lungs' intrinsic defenses with a unique combination of inhaled Toll-like receptor (TLR) agonists broadly protects mice against otherwise lethal pneumonias. As the survival benefit persists despite cytotoxic chemotherapy-related neutropenia, the cells required for protection were investigated. The inducibility of resistance was tested in mice with deficiencies of leukocyte lineages due to genetic deletions and in wild-type mice with leukocyte populations significantly reduced by antibodies or toxins. Surprisingly, these serial reductions in leukocyte lineages did not appreciably impair inducible resistance, but targeted disruption of TLR signaling in the lung epithelium resulted in complete abrogation of the protective effect. Isolated lung epithelial cells were also induced to kill pathogens in the absence of leukocytes. Proteomic and gene expression analyses of isolated epithelial cells and whole lungs revealed highly congruent antimicrobial responses. Taken together, these data indicate that lung epithelial cells are necessary and sufficient effectors of inducible resistance. These findings challenge conventional paradigms about the role of epithelia in antimicrobial defense and offer a novel potential intervention to protect patients with impaired leukocyte-mediated immunity from fatal pneumonias.

INTRODUCTION

Lower respiratory tract infections constitute a tremendous worldwide public health threat, affecting hundreds of millions of people annually.^{1–4} Patients with hematological malignancies, those with advanced HIV disease, and certain transplant recipients face extreme pneumonia risks due to impaired leukocyte-mediated immunity.^{5–7} In fact, in the transfusion era, pneumonia is the primary cause of death among patients with leukemia.^{8,9}

We have previously reported that the lungs' mucosal defenses can be stimulated to protect mice against otherwise lethal pneumonias.^{10–14} This phenomenon, known as inducible resistance, results from inhaled treatments targeting pattern recognition receptors in the lungs and yields broad protection against bacterial, viral, and fungal pathogens.^{10,13,15–17} Most recently, we showed that robust pneumonia protection could be induced by a single inhaled treatment consisting of a unique,

synergistic combination of Toll-like receptor (TLR) agonists: a diacylated lipopeptide ligand for TLR2/6, Pam2CSK4, and a class C unmethylated 2'-deoxyribo cytidine-phosphate-guanosine ligand for TLR9, oligonucleotide (ODN) M362 (hereafter, 'Pam2-ODN').^{15,17}

Notably, although we have shown that onset of protection temporally correlates with treatment-induced neutrophil influx into the lungs, we have also demonstrated persistent protection, despite profound depletion of neutrophils and macrophages.^{10,11,15} As these leukocytes are widely considered the primary mediators of mucosal immunity in the lungs, these findings raised the question of which cells are principally required for inducible resistance.

Although the airway and alveolar epithelia are often regarded as passive airflow conduits and inert gas exchange barriers, it is evident that they possess intrinsic antimicrobial capacity that contributes to pathogen clearance under physiological

¹Department of Pulmonary Medicine, The University of Texas MD Anderson Cancer Center, Houston, Texas, USA. ²Tecnológico de Monterrey School of Medicine, Monterrey, Nuevo León, Mexico. ³Department of Bioinformatics and Computational Biology, The University of Texas MD Anderson Cancer Center, Houston, Texas, USA. ⁴Center for Infectious and Inflammatory Disease, Institute of Biosciences and Technology, Texas A & M Health Science Center, Houston, Texas, USA. ⁵Division of Pulmonary Disease and Critical Care, University of Vermont College of Medicine, Burlington, Vermont, USA and ⁶University of Texas Graduate School of Biomedical Science, Houston, Texas, USA. Correspondence: SE Evans (seevans@mdanderson.org)

Received 30 August 2012; accepted 22 March 2013; advance online publication 1 May 2013. doi:10.1038/mi.2013.26

conditions.^{12,18–22} The current work supports an essential role for the lung epithelium in the therapeutic induction of resistance,^{10–12,15} but surprisingly, does not clearly identify any individual leukocyte lineages that are required for protection. These findings not only challenge conventional paradigms about the role of the lung epithelium in antimicrobial defense but also offer the potential to protect vulnerable patients with impaired leukocyte-dependent immunity.

RESULTS

Pam2-ODN-induced resistance to pneumonia persists despite reductions in numerous leukocyte lineages

Leukocytes are generally viewed as the principal (or sole) mediators of pulmonary innate immunity. However, as we have reported durable anti-pneumonia protection following leukocyte-depleting therapies,^{10,15} we serially depleted leukocyte lineages in an effort to determine which cell types were required for inducible resistance.

Consistent with previous observations using myeloablative therapies,¹⁵ depletion of neutrophils to undetectable levels in both blood and bronchoalveolar lavage fluid (BALF; **Supplementary Figure S1A** online) failed to impair Pam2-ODN-induced protection against otherwise lethal infections with *Pseudomonas aeruginosa* and *Streptococcus pneumoniae* (**Figure 1a,b**). Further, neutrophil-depleted lungs could still be induced to kill bacteria by a single inhaled Pam2-ODN treatment. Although complete absence of neutrophils is not assumed to occur following antibody-mediated depletion, no recruitable neutrophils were detected in the lungs of antibody-treated mice in the first 12 h after pathogen challenge, despite the observed differences in pathogen burden starting immediately after infection. By 24 h after pathogen challenge, rare neutrophils could be detected in the lungs of surviving mice by flow cytometry, though at a greatly reduced level compared with undepleted mice (**Supplementary Figure S1B** online).

To address the role of alveolar macrophages in inducible resistance, mice were treated with intratracheal liposomal clodronate, resulting in 70–80% reductions in alveolar macrophages in the airways of treated mice compared with untreated mice or mice treated with control liposomes. Mice depleted of alveolar macrophages in this manner displayed no impairment in either Pam2-ODN-induced protection or rapid intrapulmonary pathogen killing (**Figure 1c**). Similarly, mice lacking functionally mature lymphocytes (**Figure 1d**) displayed no impairment of inducible resistance.

Dendritic cells have been reported to critically participate in modulation of mucosal defense in the lungs and elsewhere,^{23,24} and they express abundant TLRs.^{25,26} Therefore, these lineages were viewed as likely to be required for Pam2-ODN-induced resistance. However, despite substantial reductions in the number of conventional dendritic cells with diphtheria toxin or antibody-mediated depletion of plasmacytoid dendritic cells (**Supplementary Figure S2** online), mice were still protected against lethal *Pseudomonas* pneumonia (**Figure 1e,f**).

Protection was equally inducible by Pam2-ODN in mice substantially depleted of dendritic cells and in sham-depleted mice.

Given their microbicidal role in innate immunity,^{27,28} natural killer (NK) cells were also investigated as potential mediators of inducible resistance. However, mice significantly depleted of NK cells with antibodies (**Supplementary Figure S2** online) and mice lacking functional NK cells due to perforin deficiency similarly displayed no impairment of Pam2-ODN-induced resistance (**Figure 1g,h**).

In addition to exerting directly microbicidal effects on infecting pathogens, leukocytes also express interleukin-22 (IL-22) in response to infections, promoting antimicrobial responses from non-hematopoietic cells at environmental interfaces.²⁹ Consistent with the leukocyte depletion studies, IL-22 knock-out mice were fully protected by Pam2-ODN against *P. aeruginosa* pneumonia (**Figure 2**). Taken together, these studies fail to demonstrate a single, critically important leukocyte effector of inducible resistance.

Pam2-ODN-induced resistance requires canonical TLR signaling pathway activation

As no individual leukocyte was confirmed to be a central effector cell of inducible resistance, an alternate effector cell was needed to explain the protective response induced by Pam2-ODN. We have hypothesized that lung epithelial cells might serve an effector function in inducible resistance.^{11,13,15} However, unlike the tested leukocytes, anatomical depletion of the lung epithelium is incompatible with host survival. So, it was necessary to identify a means to functionally disrupt the epithelium without impairing gas exchange.

TLR2/6:Pam2 and TLR9:ODN-initiated signaling events are described to require the Toll/IL-1 receptor adaptor myeloid differentiation primary response gene 88 (MyD88). However, given the unanticipated synergy observed with Pam2-ODN, it was important to confirm that the Pam2-ODN-induced protection actually required signal propagation via known MyD88 pathways. As shown in **Figure 3a**, although wild-type mice were fully protected against *P. aeruginosa* pneumonia by a single inhaled Pam2-ODN treatment on the day before infection, MyD88-deficient littermates could not be similarly protected. Consonantly, Pam2-ODN induced rapid pathogen killing in the lungs of *Pseudomonas*-challenged wild-type mice but had no such effect in MyD88-deficient mice.

Recent structural and functional analyses indicate that MyD88-dependent TLR signaling is propagated by formation of giant signalosomes ('Myddosomes') following recruitment of IL-1 receptor-associated kinase 4 (IRAK4).^{30–33} Given the novel synergy observed with Pam2-ODN, we sought to further test whether inducible resistance utilized this classically described TLR-MyD88-IRAK4 pathway. **Figure 3b** confirms that IRAK4-deficient mice phenocopy mice lacking MyD88, resulting in total abrogation of the protective Pam2-ODN effect against *P. aeruginosa* pneumonia and failing to induce pathogen killing in the lungs.

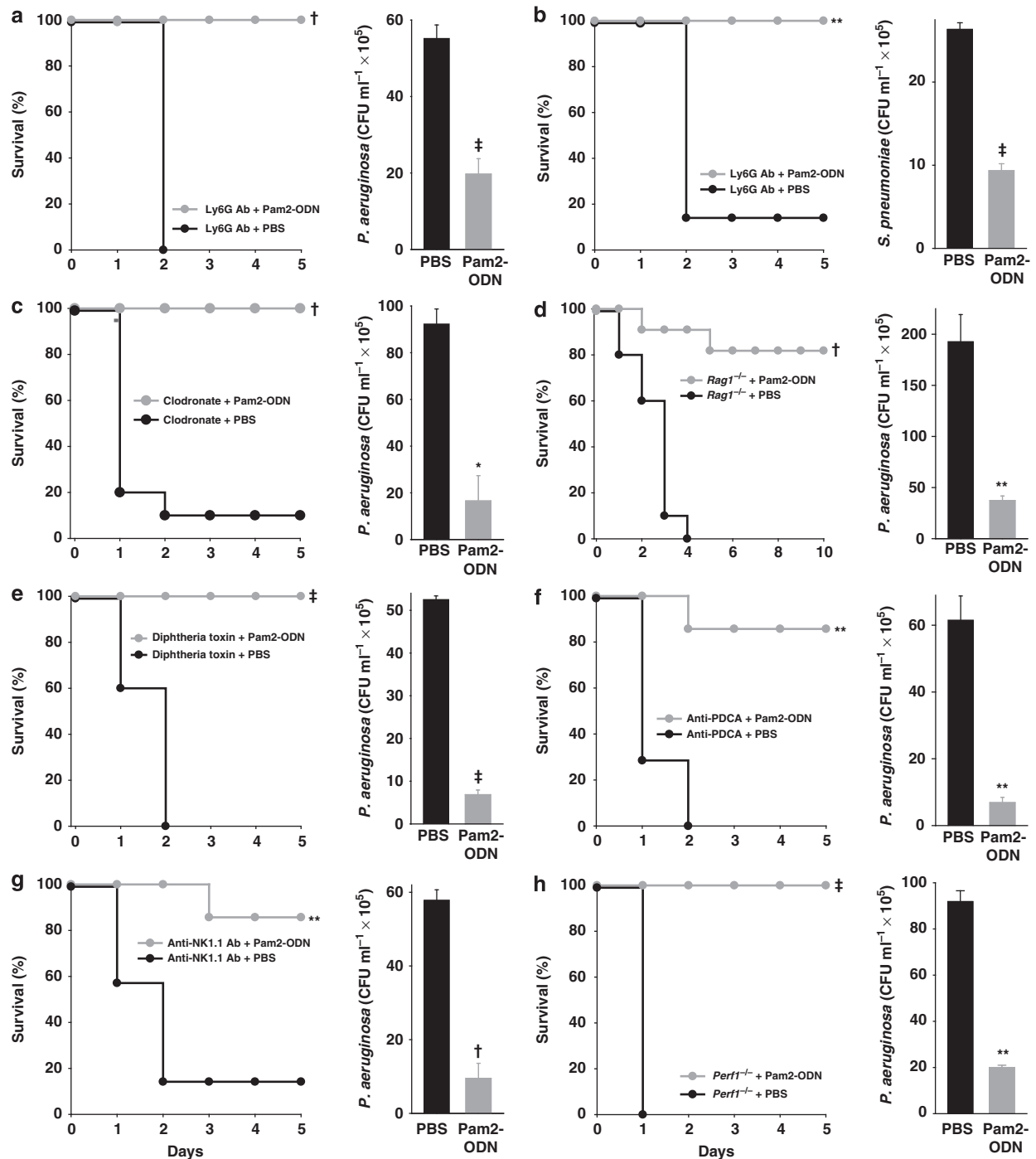


Figure 1 No leukocytes are identified to be required for Pam2-ODN-induced resistance. (a) Wild-type C57BL/6 J mice were depleted of neutrophils by intraperitoneal injection of anti-Ly6G Ab, then inhalationally challenged with *Pseudomonas aeruginosa* grown to mid-log phase following a single aerosolized treatment consisting of Pam2CSK4 and oligonucleotide (ODN) M362 (Pam2-ODN) or phosphate-buffered saline (PBS; sham) treatment of the mice 24 h before the infectious challenge. (b) Neutrophil-depleted mice were inhalationally challenged with *Streptococcus pneumoniae* in mid-log phase with or without aerosolized Pam2-ODN pretreatment 24 h before infection. (c) Wild-type mice were depleted of alveolar macrophages by two intratracheal treatments with liposomal clodronate before challenge with *P. aeruginosa* with or without aerosolized Pam2-ODN pretreatment 24 h before infection. (d) *Rag1*^{-/-} mice were challenged with *P. aeruginosa* with or without aerosolized Pam2-ODN pretreatment 24 h before infection. (e) Mice expressing the diphtheria toxin receptor under the *CD11c* promoter received repetitive intratracheal doses of diphtheria toxin before challenge with *P. aeruginosa* with or without aerosolized Pam2-ODN pretreatment 24 h before infection. (f) Wild-type mice were depleted of plasmacytoid dendritic cells by intraperitoneal injection with anti-PDCA Ab before challenge with *P. aeruginosa* with or without aerosolized Pam2-ODN pretreatment 24 h before infection. (g) Wild-type mice were depleted of natural killer cells by intraperitoneal injection with anti-NK1.1 Ab before challenge with *P. aeruginosa* with or without aerosolized Pam2-ODN pretreatment 24 h before infection. (h) *Perfl*^{-/-} mice were challenged with *P. aeruginosa* with or without aerosolized Pam2-ODN pretreatment 24 h before infection. For all the experiments, the left panel displays pneumonia survival ($N = 8-10$ mice/group for all the experiments), the right panel displays the lung pathogen burden immediately after the infectious challenge as assessed by serial dilution culture of whole lung homogenates ($N = 3-6$ mice/group for all the experiments). Panels shown are representative of at least three separate experiments. All the survival groups were followed for at least 14 days, no deaths occurred outside the presented periods. (* $P < 0.03$, ** $P < 0.005$, † $P < 0.0006$, ‡ $P < 0.00001$ relative to PBS-treated control). CFU, colony-forming units.

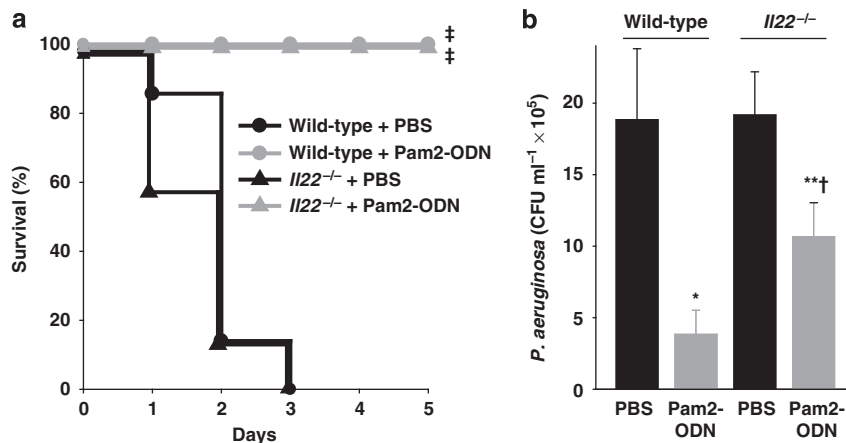


Figure 2 Interleukin (IL)-22 is not required for Pam2-ODN-induced resistance. *Il22*^{-/-} mice and wild-type littermates were inhalationally challenged with *Pseudomonas aeruginosa* grown to mid-log phase with or without aerosolized Pam2-ODN (oligonucleotide) pretreatment 24 h before the infectious challenge. (a) Survival of pneumonia ($N=8$ mice/group), (b) lung pathogen burden immediately after the infectious challenge as assessed by serial dilution culture of whole lung homogenates ($N=3$ mice/group). (* $P<0.01$ vs. phosphate-buffered saline (PBS)-treated wild-type; ** $P<0.03$ vs. PBS-treated *Il22*^{-/-}; † $P>0.09$ vs. Pam2-ODN-treated wild-type; ‡ $P<0.0001$ vs. PBS-treated syngeneic mice). CFU, colony-forming units.

Although we have described broad protection following Pam2-ODN treatment, it is conceivable that protection against different pathogens occurs via different mechanisms. To confirm that protection against non-*Pseudomonas* pathogens proceeds via recruitment of the same proximal signaling molecules, we also attempted to induce protection against a Gram-positive bacterium and a virus by Pam2-ODN inhalation in IRAK4-deficient mice. As shown, Pam2-ODN protects wild-type mice against lethal challenge with these pathogens, but IRAK4 deficiency resulted in complete loss of inducible resistance against *S. pneumoniae* (Figure 3c) and influenza A (Figure 3d).

Lung epithelial cells are necessary and sufficient for inducible resistance

The requirement for canonical TLR-MyD88-IRAK4 signaling following Pam2-ODN inhalation afforded an opportunity to functionally disrupt the epithelium without requiring cellular depletion. So, MyD88 was conditionally deleted in lung epithelial cells. As observed in experiments with full MyD88 knock-out mice (Figure 3a), inhaled Pam2-ODN treatment conferred no significant protection to lung epithelium-specific *Myd88*^{SPCΔ/Δ} mice challenged with *P. aeruginosa* (Figure 4a) nor could intrapulmonary pathogen killing be induced by the TLR treatment (Figure 4b). Similarly, as shown in Figure 4c, protection against lethal influenza pneumonia by Pam2-ODN was also found to be highly dependent on lung epithelial MyD88. Together, these studies confirm that MyD88-dependent signaling in the lung epithelium is required for Pam2-ODN-induced resistance to pneumonia.

Pam2-ODN-induced protection is described as inducible resistance, rather than inducible tolerance, because the survival benefit is consistently associated with reductions in pathogen burden. Remarkably, inducible pathogen killing is even evident immediately after delivery of an infectious challenge. As shown

in Figure 5a, the lungs of Pam2-ODN-treated wild-type mice contained one log fewer *P. aeruginosa* CFU ml⁻¹ than did sham-treated mice immediately after inhalational challenge. Twenty-four hours after infection, the lung pathogen burden of the sham-treated mice had again doubled, whereas Pam2-ODN-treated mouse lungs demonstrated a bacterial burden reduced by another two logs compared with Pam2-ODN-treated mice at 0 h. By 48 h after infection, the Pam2-ODN-treated mice cleared the remaining pathogens, whereas the sham-treated mice had all succumbed to infection. Together, these data suggest that generation of a microbicidal environment is an important, ongoing process in effective inducible resistance.

Testing the sufficiency of lung epithelial cells to generate such a microbicidal environment, isolated lung epithelial cells were stimulated with Pam2-ODN for 4 h before bacterial infection. Pam2-ODN-treated primary mouse tracheal epithelial cells infected with luminescent *S. pneumoniae* demonstrated significantly lower pathogen burdens than did phosphate-buffered saline (PBS)-treated controls, as assessed by luminescence intensity (Figure 5b). We and others have previously reported that culture luminescence correlates with an extremely high degree of certainty ($R^2>0.998$) with pathogen burden as assessed by serial dilution cultures, and allows for detection of free, bound, and internalized pathogens.^{15,34,35} Thus, Pam2-ODN-treated epithelial cells appeared to autonomously reduce the pathogen burden. However, because it is virtually impossible to exclude the possibility of leukocyte contamination in primary epithelial cultures, we also tested a model system that allowed for no such contamination. Using the human bronchial epithelial cell line HBEC3-KT,³⁶ we observed comparable induction of pathogen killing by epithelial cells in the absence of any leukocytes (Figure 5c).

Further exploring the capacity of epithelial cells to mediate the observed protective response, we compared Pam2-ODN-

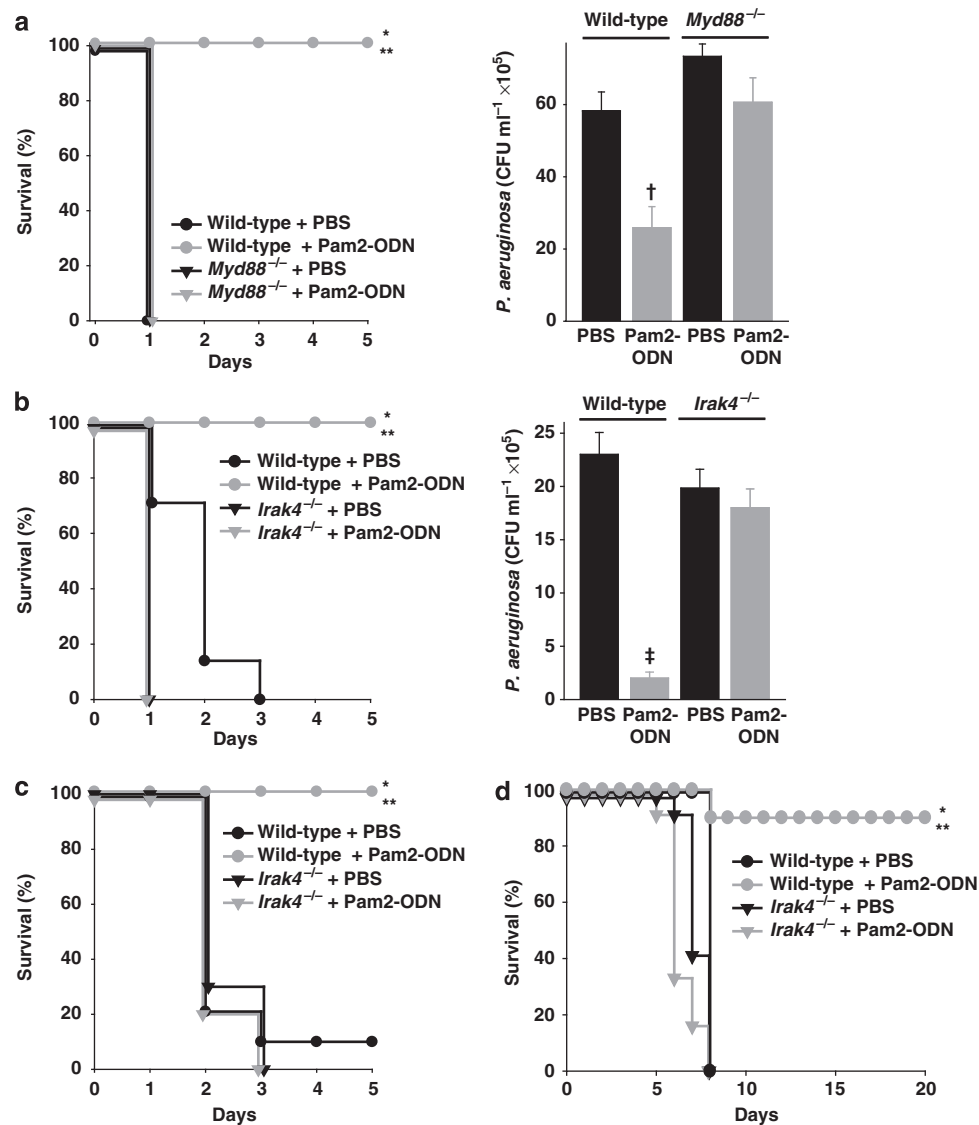


Figure 3 Myeloid differentiation primary response gene 88 (Myd88) and interleukin-1 receptor-associated kinase 4 (IRAK4) are required for Pam2-ODN-induced resistance. (a) *Myd88*^{-/-} and wild-type littermates were inhalationally challenged with *Pseudomonas aeruginosa* grown to mid-log phase with or without aerosolized Pam2-ODN (oligonucleotide) treatment 24 h before infection. Left, survival ($N = 10$ mice/group); right, lung bacterial burden immediately after infection ($N = 3$ mice/group). (b) *Irak4*^{-/-} and wild-type mice inhalationally challenged with *P. aeruginosa* with or without Pam2-ODN pretreatment 24 h before infection. Left, survival ($N = 10$ mice/group); right, lung bacterial burden immediately after infection ($N = 3$ mice/group). (c) *Irak4*^{-/-} and wild-type mice inhalationally challenged with *Streptococcus pneumoniae* with or without Pam2-ODN pretreatment 24 h before infection. (d) *Irak4*^{-/-} and wild-type mice inhalationally challenged with influenza A virus (H3N2) with or without Pam2-ODN pretreatment 24 h before infection. (* $P < 0.0001$ wild-type + Pam2-ODN vs. knock-out + Pam2-ODN; ** $P < 0.0001$ wild-type + PBS (phosphate-buffered saline) vs. wild-type + Pam2-ODN; † $P < 0.02$ wild-type + PBS vs. wild-type + Pam2-ODN). CFU, colony-forming units.

induced gene expression in isolated mouse lung epithelial cells (MLE-15) to that of whole mouse lung homogenates. By hypergeometric testing,^{37,38} the two gene sets were found to significantly overlap ($P < 10^{-10}$), indicating that lung epithelial cells (in the absence of leukocytes) respond to Pam2-ODN exposure in a manner that was statistically similar to intact mouse lungs treated with Pam2-ODN. **Figure 5d** shows the 585 congruently differentially expressed transcripts, not surprisingly heavily enriched for TLR signaling and antimicrobial defense genes (individually reported in **Supplementary Table S1** online).

Previous proteomic analyses demonstrate antimicrobial peptide production following inhalation of bacterial lysates.¹⁰ However, we have not previously confirmed that Pam2-ODN-induced defense transcript enrichment translated into antimicrobial peptide production. Serum amyloid A3 (*Saa3*) is among the most strongly induced transcripts following lysate¹¹ or Pam2-ODN exposure,¹⁵ and it is the single most synergistically induced gene product (i.e., the greatest mRNA induction following combined Pam2-ODN treatment relative to the sum of the effects of Pam2 and ODN administered alone). As shown in **Figure 5e**, *Saa3* gene expression correlates tightly with BAL

concentrations of SAA3 protein, demonstrating both the translation of the gene expression signal and the similarity to lysate-induced resistance. Similar responses were observed for isolated MLE-15 cells (not shown).

In addition to protein mediators of resistance, we have speculated that reactive oxygen species (ROS) are generated in response to Pam2-ODN treatment but have not previously demonstrated this element of the response. Using 2',7'-dichlorodihydrofluoresceindiacetate acetyl ester (H₂DCF-DA) to detect

ROS generation, we found significant induction from MLE-15 cells within minutes of Pam2-ODN treatment (Figure 5f). To determine whether this phenomenon extended to the intact lung, we devised a novel strategy to assess for volatile ROS. Mice underwent BAL with the ROS-detecting agent L-012 added to the PBS lavagate. As shown in Figure 5g, ROS levels were significantly elevated 24 h after Pam2-ODN inhalation, and this was further enhanced in the presence of *P. aeruginosa* (but not by infectious challenge alone).

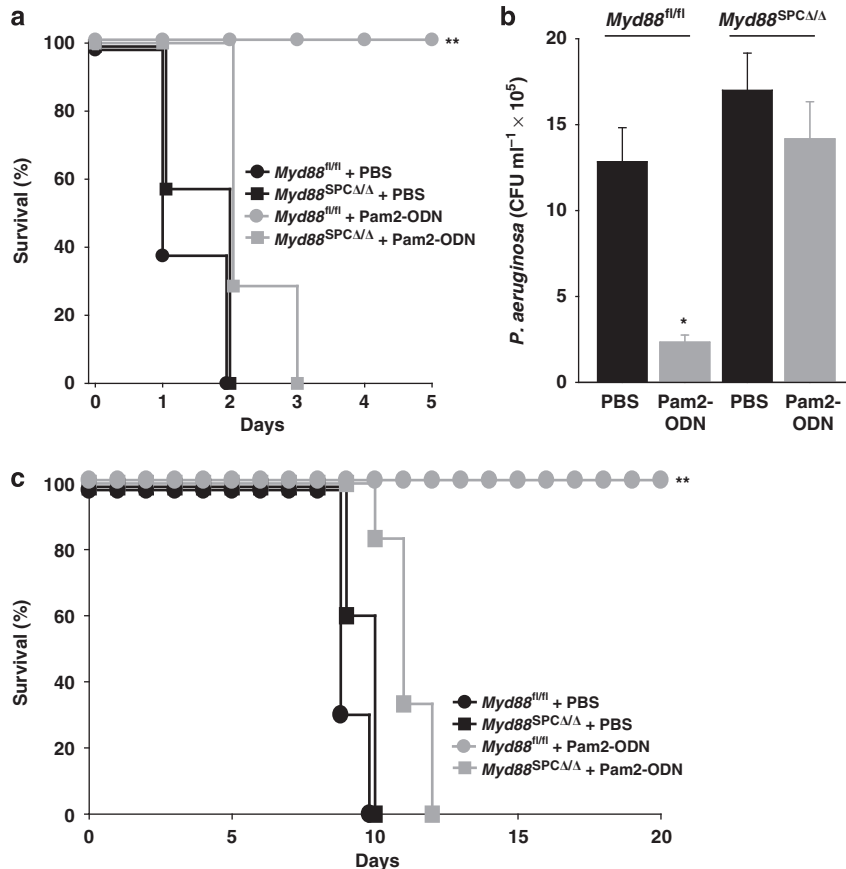


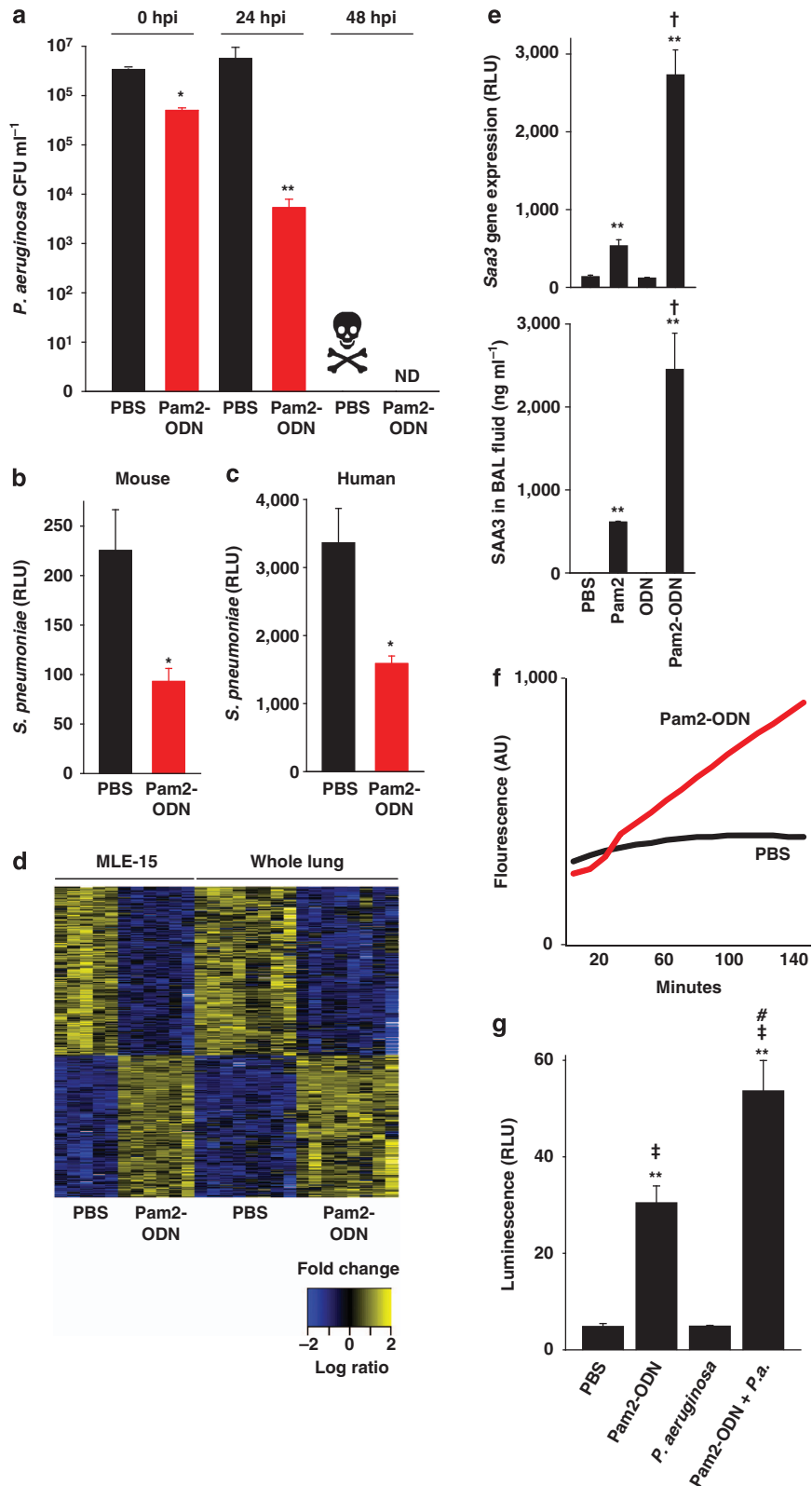
Figure 4 Lung epithelial myeloid differentiation primary response gene 88 (MyD88) is required for inducible resistance. Mice conditionally deficient in lung epithelial *Myd88* (*Myd88*^{SPCA/Δ}) and littermate controls (*Myd88*^{fl/fl}) were inhalationally challenged with *Pseudomonas aeruginosa* grown to mid-log phase with or without aerosolized Pam2-ODN (oligonucleotide) pretreatment 24 h before the infectious challenge: (a) pneumonia survival (*N* = 8 mice/group), and (b) lung pathogen burden immediately after the infectious challenge (*N* = 3 mice/group). (c) Survival of influenza pneumonia in lung epithelial *Myd88* deletants and littermate controls with or without aerosolized Pam2-ODN pretreatment 24 h before the infectious challenge. (**P* < 0.0005 vs. phosphate-buffered saline (PBS)-treated *Myd88*^{fl/fl}; ***P* < 0.0001 vs. Pam2-ODN-treated *Myd88*^{SPCA/Δ}). CFU, colony-forming units.

Figure 5 Pam2-ODN (oligonucleotide) induces antimicrobial responses from isolated epithelial cells. (a) Wild-type mice were inhalationally challenged with *Pseudomonas aeruginosa* grown to mid-log phase with or without aerosolized Pam2-ODN treatment 24 h before infection. Lungs were harvested at the indicated times after infection, homogenized in 1 ml phosphate-buffered saline (PBS), and submitted to serial dilution culture. All sham-treated mice died before the 48-h harvest. (*N* = 3–6 mice/group). (b) Primary mouse tracheal epithelial cell cultures were inoculated with luminescent *Streptococcus pneumoniae* 4 h after pretreatment with Pam2-ODN or PBS, then the culture pathogen burden was assessed by luminescence intensity. (c) Pathogen burden of HBEC3-KT cultures infected with luminescent *S. pneumoniae* 4 h after pretreatment with Pam2-ODN or PBS. (d) Heat map of differentially expressed genes in MLE-15 (mouse lung epithelial cells) or whole mouse lung homogenates 4 h after treatment with Pam2-ODN, shown as standardized log ratios of fold change. (e) Serum amyloid A3 (*Saa3*) mRNA levels in whole lung homogenates (upper panel) and SAA3 protein concentration in bronchoalveolar lavage (BAL) fluid (lower panel). (f) Reactive oxygen species generation by MLE-15 cells following treatment with PBS or Pam2-ODN, detected by H₂DCF-DA (2',7'-dichlorodihydrofluoresceindiacetate acetyl ester). (g) Reactive oxygen species generation by intact lungs, assessed by luminescence detection of BAL fluid following lavage with L-012-containing PBS. (hpi, hours post-infection; ND, none detected; **P* < 0.04 vs. PBS-treated; ***P* < 0.008 vs. PBS-treated; †*P* < 0.008 vs. Pam2-treated; ‡*P* < 0.001 vs. *P. aeruginosa*-infected; #*P* < 0.035 vs. Pam2-ODN-treated, uninfected). AU, arbitrary units; CFU, colony-forming units; RLU, relative light units.

DISCUSSION

Pneumonia remains a leading cause of death in virtually all populations worldwide. Our recent reports have described the novel strategy of therapeutically stimulating the lungs' intrinsic

defenses as a means to counter this threat. Although we have previously hypothesized that the epithelium could have an important role in facilitating inducible resistance, we have heretofore been unable to conclusively demonstrate the



contribution of the epithelia to inducible resistance. The data presented here allow us, for the first time, to convincingly demonstrate an essential role for lung epithelial cells as essential effectors of inducible resistance.

Therapy-induced leukocyte infiltration of the lungs, particularly neutrophil influx, has been temporally associated with the onset of inducible resistance. However, we previously identified instances where protection persisted despite neutrophil depletion.^{10,15} In the current study, serial reductions of several leukocyte populations did not reveal any individual hematopoietic cell types that were definitely required for Pam2-ODN-induced resistance. As the antibody- and toxin-dependent leukocyte-depleting techniques used may fail to achieve complete absence of their target populations, it is difficult to conclusively infer the role of individual leukocytes from the depletion studies when considered in isolation. Moreover, we hypothesize that leukocytes, when present, likely provide a reinforcing signal that promotes inducible resistance, at a minimum. Nonetheless, it is notable that protection can still be induced in mice substantially depleted of multiple leukocyte types.

This finding is of potentially great importance to numerous immunocompromised patient populations. Many patients with hematological malignancies, autoimmune diseases, advanced HIV disease, and solid organ or stem cell transplants face elevated risks of pneumonia due to quantitative or qualitative leukocyte deficiency. If inducible resistance relied heavily on these deficient cells, aggressive inhalational stimulation with Pam2-ODN would be unlikely to benefit the most vulnerable patients. Therefore, leukocyte independence of the protective response would be a highly favorable characteristic for these immunocompromised populations.

Potentially limiting the interpretation of these results is that, in most experiments, only one leukocyte lineage was depleted at a time. Although most conditions do not present with pan-leukocyte depletion, it is conceivable that concurrently depleting multiple cell types could result in an uncompensatable defect or otherwise impair the Pam2-ODN response. Further, it is possible that differences in the duration and means of leukodepletion might influence a defect of inducible resistance, and this is an area of ongoing research. However, as IL-22 has been shown to be a critical means for leukocyte-mediated stimulation of epithelia and as we have found IL-22 to be dispensable for inducible resistance, it appears less likely that a combination of leukocyte deficiencies would further impair this epithelial response. Moreover, the demonstration of antimicrobial responses from isolated epithelial cells emphasizes the importance of leukocyte-independent epithelial responses in Pam2-ODN-induced protection.

The identification of the epithelium as a critical mediator of inducible resistance is also a favorable finding from the perspective of protecting immunocompromised patients. Suppression of leukocyte-mediated immunity, as in hematological malignancies and/or cytotoxic chemotherapy, does not obviate the lungs' intrinsic responses to infection. Rather, profoundly immunosuppressed patients generate striking

inflammatory responses to pulmonary infections.³⁹ Perhaps more importantly, lung epithelial cells' capacity to generate antimicrobial responses are uniquely spared the effects of immunosuppressive therapy,⁴⁰ probably reflecting their slow cellular turnover rate, as contrasted with rapidly replaced gut epithelial cells that display loss of barrier and antimicrobial function with cytotoxic therapies.^{41,42} Thus, inducible epithelial resistance may liberate many patients from reliance on leukocyte-mediated immunity as their sole defense against pneumonia by engaging cells that are relatively impervious to the immunosuppressive and cytotoxic therapies they require for their underlying diseases.

We are not the first group to demonstrate active participation of epithelial cells in host defense. In fact, Mijares *et al.* have reported that lung epithelial MyD88 contributes to mouse survival in a model of *P. aeruginosa* pneumonia.⁴³ However, to our knowledge, we are the first to show that loss of MyD88 in the lung epithelium results in loss of protective immunity in the presence of an intact leukocyte-mediated immune system. Further, unlike other studies investigating TLR signaling in the lungs, we have shown a requirement for epithelial function for therapeutic enhancement of mucosal immunity, whereas others have focused on modulating baseline susceptibility to infection. Although the confirmation of MyD88-dependent signaling advances our understanding of inducible resistance, based on the unique synergy of two reportedly MyD88-dependent TLR ligands, we hypothesize that MyD88-independent events also contribute to the protective phenomenon. For instance, the current studies have not excluded the possibility of Pam2-ODN-induced signaling via TRIF (TIR-domain-containing adapter-inducing interferon- β) or inflammasome-associated pathways.

Another unique aspect of these studies is the demonstration of direct antimicrobial responses from the lung epithelium following Pam2-ODN treatment. Regardless of organ, previous reports of epithelial stimulation by TLR ligands almost all identify leukocytes as the primary TLR target cells, with subsequent (leukocyte-derived) cytokines driving epithelial responses. By apparently obviating the need for an intermediary leukocyte, this may expand the pool of potentially benefitting patients to include those without functional leukocytes and could afford an immense targetable surface area ($\sim 100\text{ m}^2$) for delivery of the inhaled therapeutic.

Pam2-ODN-enhanced survival of pneumonia consistently correlates with the generation of an antimicrobial environment, resulting in rapid induction of pathogen killing at the time of infection. As shown in **Figures 1–5**, lungs of Pam2-ODN-treated mice harvested immediately after delivery of an infectious challenge demonstrate significantly lower pathogen burdens than lungs of sham-treated mice. Whether the relatively modest differential between the initial pathogen burdens of Pam2-ODN-treated and sham-treated lungs fully accounts for the survival benefit is unknown, but it is suspected that this initial antimicrobial response is only one contributor to protection. Whereas these

earliest antimicrobial effects may reflect release of preformed stores of effector molecules and/or activation of existing ROS generators, later effects may reflect transcriptionally regulated production of microbicidal molecules, modulation of host molecules that facilitate pathogen adherence or invasion, enhancements of mechanical barrier function, and increased mucociliary clearance of pathogens and noxious debris. Ongoing pathogen killing, containment, and clearance are suggested by the dramatic widening of the pathogen differential in the lungs at later time points (Figure 5a) and the prevention of septicemia by Pam2-ODN treatment (Supplementary Table S2 online).

Although we have demonstrated production of both antimicrobial peptides and ROS by the epithelium, the current studies do not attempt to ascertain which molecules are required for the antimicrobial response. However, our identification of a required cellular compartment is expected to facilitate the necessary studies to discover the critical effector molecules, particularly when integrated with novel mutant mouse models presently in development. We have reported SAA3 to be the most synergistically induced antimicrobial molecule in the lung following Pam2-ODN treatment. Previously, we reported that the inducible SAA proteins also comprised three of the four most upregulated transcripts following resistance-inducing treatment with inhaled bacterial lysates.¹¹ Locally produced SAA proteins have been reported to exert direct antimicrobial effects, to promote ROS generation, to facilitate the phagocytosis of certain bacteria, to promote the recruitment and activation of myeloid cells, and to polarize T helper type 17 immune responses.^{44–47} Consequently, lung epithelial induction of SAA3 is an attractive target for therapeutic manipulation and may be an important contributor to Pam2-ODN-induced protection.

Together, these data provide critical insights into the mechanisms of inducible resistance. By establishing the central role of lung epithelial cells in the antimicrobial response, these data provide an opportunity to develop more accurate models to explore the means by which the lungs' inherent defenses can be exploited to kill pathogens. More urgently, these data provide hope that we can utilize this technology to protect our patients during periods of peak vulnerability.

METHODS

Animals and reagents. All general reagents were obtained from Sigma-Aldrich (St Louis, MO), except as indicated. All mice were handled in accordance with the Institutional Animal Care and Use Committee of The University of Texas MD Anderson Cancer Center. Mouse experiments were performed with 5–8-week-old mice. Unless indicated, C57BL/6J mice (The Jackson Laboratory, Bar Harbor, ME) were used. To eliminate intergroup variability, all mice in each experiment were of a single gender. *Rag1*^{-/-}, *CD11c*-DTR, and *Perf1*^{-/-} mice were purchased from Jackson. *Myd88*^{-/-} mice⁴⁸ were provided by Shizuo Akira. *Irak4*^{-/-} mice⁴⁹ were provided by Wen-Chen Yeh (Amgen, Thousand Oaks, CA). *Il22*^{-/-} mice⁵⁰ were provided by Wenjun Ouyang (Genentech, South San Francisco, CA). Mice with *LoxP* sites flanking exon 3 of *Myd88*⁵¹ were provided by Anthony L. DeFranco. *Sftpc*-Cre mice⁵² were provided by Brigid L. M. Hogan.

Aerosol treatments. S-[2,3-bis(palmitoyloxy)-propyl]-(R)-cysteinyl-(lysyl) 3-lysine (Pam2CSK4) and ODN M362 (InvivoGen, San Diego, CA) were reconstituted in endotoxin-free water and suspended in sterile PBS. As described,¹⁵ the Pam2-ODN was placed in an Aerotech II nebulizer (Biodex Medical Systems, Shirley, NY) driven by 10 l min⁻¹ air supplemented with 5% CO₂ for 20 min. The nebulizer was connected by polyethylene tubing to a polyethylene exposure chamber.

Infection models. As described,^{10,11,13,15} mice were challenged inhalationally with bacterial inocula targeted to a dose lethal to 90–100% of the infected mice (LD₉₀–LD₁₀₀). Frozen stock of *P. aeruginosa* strain PA103 (American Type Culture Collection, Manassas, VA) was incubated for 16 h in 200 ml Luria-Bertani medium at 37 °C in 5% CO₂, then diluted in 1.5 l fresh broth, and grown at 37 °C to an OD₆₀₀ (optical density at wavelength of 600 nm) of 0.5, yielding 1–4 × 10¹⁰ CFU ml⁻¹. Frozen stock of a mouse-adapted clinical isolate of *Streptococcus pneumoniae* serotype 4 was incubated for 16 h in 200 ml Todd-Hewitt broth at 37 °C in 5% CO₂, then diluted in 1.5 l fresh broth, and grown to an OD₆₀₀ target of approximately 0.5, yielding 2–6 × 10¹¹ CFU ml⁻¹. The bacterial suspensions were centrifuged, washed, resuspended in 10 ml PBS, and aerosolized over a period of 60 min in the exposure chamber. To determine lung pathogen burdens, mouse lungs were harvested under anesthesia immediately after infections and homogenized in 1 ml sterile PBS with 1 g of sterile glass beads using a Mini-Beadbeater-1 (Biospec, Bartlesville, OK). Serial dilutions of challenge inocula and lung homogenates were plated on tryptic soy agar plates (Becton Dickinson, Franklin Lakes, NJ), incubated at 37 °C for 16 h, and bacterial CFUs were counted.

Frozen stock (2.8 × 10⁷ TCID₅₀ ml⁻¹) of mouse-adapted influenza A/Hong Kong/8/68 (H3N2; Mouse Lung Pool 1-17-12 provided by Brian E. Gilbert)⁵³ was diluted 1:250 in 0.05% gelatin in Eagle's minimal essential medium and aerosolized for 20 min to achieve LD₉₀–LD₁₀₀ (target 100 TDIC₅₀ per mouse). Viral concentrations in the nebulizer before and after aerosolization were determined by hemagglutination assay of infected MDCK cells.⁵⁴

Leukocyte-depletion models. Neutrophils were depleted by injecting 100 µl anti-Ly6G mAb (clone RB6-8C5) intraperitoneally one day before Pam2-ODN treatment. Alveolar macrophages were depleted by intratracheal administration of 50 µl liposomal clodronate (0.25 g ml⁻¹, provided by Nico van Roojen) on days -3 and -2 before infection. Conventional dendritic cells and CD11c-expressing monocytes/macrophages were depleted in the lungs by administering 50 µl diphtheria toxin intranasally to *CD11c*-DTR mice on days -2 and -1 before infection. Plasmacytoid dendritic cells were depleted by injecting 100 µl anti-PDCA mAb (clone JF05-1C2.4.1, Miltenyi, Bergisch Gladbach, Germany) intraperitoneally on days -2 and -1 before Pam2-ODN treatment. NK cells were depleted by injecting 100 µl anti-Nk1.1 mAb (clone PK136, Pierce Antibodies, Rockford, IL) intraperitoneally on days -2 and -1 before Pam2-ODN treatment.

To confirm peripheral depletion of neutrophils, blood samples were obtained from the inferior vena cavae of anesthetized mice using 1-ml syringes containing sodium citrate. To confirm depletion of CD11c+ cells, plasmacytoid dendritic cells, and NK cells, mouse lungs were harvested, minced, and disaggregated with collagenase and DNase I. Blood and lung samples were then treated with red blood cell lysis buffer before flow cytometry using a Becton Dickinson LSR II Laser Flow Cytometer as described.^{10,11,55} For BAL cytology, fluid was obtained by instilling and collecting two aliquots of 1 ml each of PBS through a luer stub adapter cannula (Becton Dickinson) inserted through rings of the exposed trachea at indicated time points. Total leukocyte count was determined with a hemacytometer (Hauser Scientific, Horsham, PA) and differential count by cytocentrifugation of 300 µl of BALF followed by Wright–Giemsa staining.

In vitro pathogen killing assays. To test pathogen killing by epithelial cells, mouse tracheal epithelial cells were isolated as described.⁵⁶

Briefly, mouse tracheas were digested overnight with 0.15% pronase (Roche, Tucson, AZ). Disaggregated cells were incubated in Ham's F12/DMEM (Dulbecco's modified Eagle's medium; Invitrogen) containing 4 mM glutamine (Invitrogen), 10 units penicillin-streptomycin, 0.25 $\mu\text{g ml}^{-1}$ amphotericin B (Fisher Scientific, Houston, TX), and 50 $\mu\text{g ml}^{-1}$ gentamicin (Fisher Scientific) at 37 °C in 5% CO₂ for 5 h. After incubation, floating cells were collected and 3.8×10^5 cells per well were plated on collagen I/III coated 24-well tissue culture plates in Ham's F12/DMEM containing 5% heated, inactivated fetal calf serum, 4 mM glutamine, 10 units penicillin-streptomycin, 0.25 $\mu\text{g ml}^{-1}$ amphotericin B, 50 $\mu\text{g ml}^{-1}$ gentamicin, 10 $\mu\text{g ml}^{-1}$ insulin, 30 $\mu\text{g ml}^{-1}$ bovine pituitary extract (Lonza), 5 $\mu\text{g ml}^{-1}$ human transferrin (Fisher Scientific), 0.1 $\mu\text{g ml}^{-1}$ cholera toxin, 25 ng ml⁻¹ epidermal growth factor (Fisher Scientific), and 10⁻⁸ M retinoic acid. The cells were then incubated at 37 °C in 5% CO₂ for 3–4 days until confluent. To test killing by human epithelial cells, HBEC3-KT cells³⁶ (provided by John Minna) were grown in monolayer to ~80% confluence in Keratinocyte-SFM media (Invitrogen) containing bovine pituitary extract, epidermal growth factor, and 1% penicillin-streptomycin.

Epithelial cells were treated with 20 μl PBS or 20 μl of ODN M362 (20 $\mu\text{g ml}^{-1}$) and Pam2CSK4 (10 $\mu\text{g ml}^{-1}$) in antibiotic-free mouse tracheal epithelial cell culture media. Four hours later, the wells were infected with 150 CFU luminescent *S. pneumoniae* (provided by Jon McCullers). Culture luminescence was measured after infection by a Synergy 2 plate reader (Biotek, Winooski, VT).

Gene expression analysis. For *in vitro* analyses, MLE-15 cells were grown in monolayer to approximately 80% confluence, the designated treatments were added to the culture media for 4 h, and the cells were collected by scraping. For *in vivo* analyses, wild-type mice were exposed to the designated treatments by aerosol, then euthanized after 4 h. The lungs were sterilely resected and mechanically homogenized. Total RNA was isolated using RNeasy Mini kit (QIAGEN, Gaithersburg, MD). cRNA was then synthesized and amplified using Illumina TotalPrep RNA amplification kits (Ambion, Foster City, CA), labeled, and hybridized onto Illumina Mouse Ref-8 v 2.0 Expression BeadChips (Illumina, San Diego, CA), then scanned on an Illumina iScan. mRNA and cRNA quality was confirmed using an Agilent 2100 Bioanalyzer (Agilent, Santa Clara, CA). Consistent with minimum information about a microarray experiment (MIAME) standards, all the primary microarray data were deposited at the NCBI Gene Expression Omnibus (GEO) (<http://www.ncbi.nlm.nih.gov/geo/>, GEO Accession GSE26864, *in vitro*, and GSE28994, *in vivo*). Primary signal intensity was normalized between and within samples, and differentially expressed genes were identified based on signal change and inter-sample variation.

Statistical analysis. Statistical analysis was performed using SPSS v19 (SAS Institute, Cary, NC). Student's *t*-test was used to compare the lung bacterial burdens between the groups. Error bars shown in all the figures represent technical replicates within the displayed experiment, rather than aggregation of experimental replicates. Percentage of mice surviving pathogen challenges was compared using Fisher's exact test on the final day of observation, and the log-rank test was used to compare the survival distribution estimated by the Kaplan–Meier method. One-way analysis of variance with Dunnett's *post hoc* test was used to compare the BALF differential counts.

Gene expression data were background corrected using the robust microarray averaging method, then transformed by taking the base-two logarithm, and quantile normalized. Analysis of the microarray output was performed using a gene-by-gene class comparison analysis of variance to identify treatment-induced changes. To adjust for multiple testing, we used a beta-uniform mixture model to estimate the false discovery rate. Tukey's honestly significant difference test was used to compare the differences between each pair of means with appropriate adjustment for multiple testing on the level of individual genes.

Serum amyloid A3 enzyme-linked immunosorbent assay. Enzyme-linked immunosorbent assay kits for measuring mouse SAA3 were from Millipore (Billerica, MA). All assays were performed in duplicate according to the manufacturer's instructions. Reported concentrations are in ng ml⁻¹ from undiluted BALF samples (PBS and ODN) or from BALF samples diluted 1:10 in assay buffer (Pam2 and Pam2-ODN).

SUPPLEMENTARY MATERIAL is linked to the online version of the paper at <http://www.nature.com/mi>

ACKNOWLEDGEMENTS

This work is supported by NIH U01 AI82226, the MD Anderson Physician-Scientist Program, NIH P30 CA016672 Cancer Center Support Grant, and NIH P50 CA100632 Leukemia SPORE.

DISCLOSURE

M.J.T. and S.E.E. are authors on a related United States patent application entitled 'Stimulation of Innate Resistance of the Lungs to Infection with Synthetic Ligands.' M.J.T. and S.E.E. own stock in Pulmotect, which holds the commercial options on these patent disclosures. The other authors declare no financial conflicts of interest.

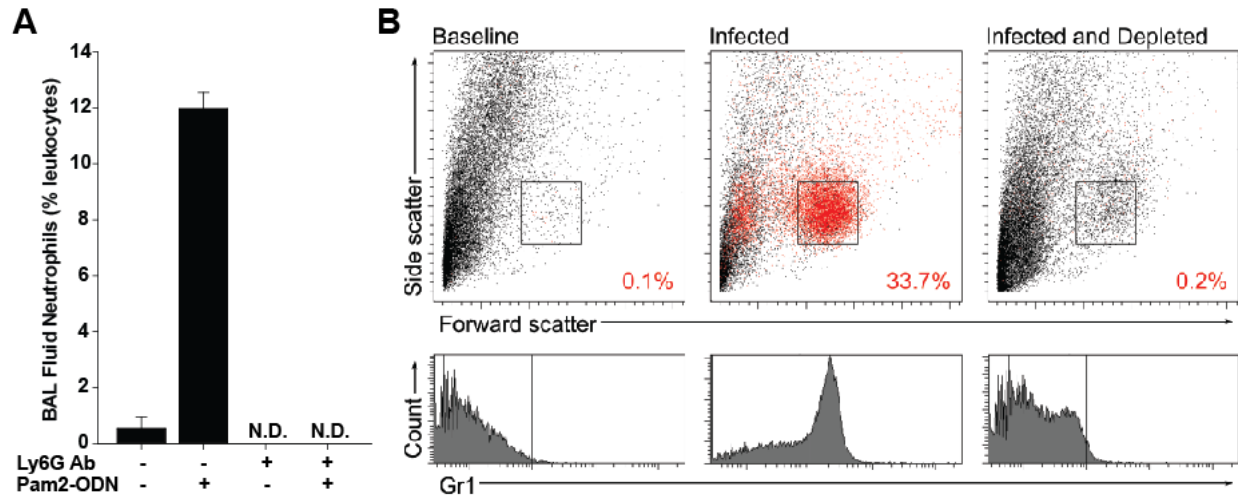
© 2013 Society for Mucosal Immunology

REFERENCES

- Mizgerd, J.P. Lung infection—a public health priority. *PLoS Med* **3**, e76 (2006).
- Morens, D.M., Folkers, G.K. & Fauci, A.S. The challenge of emerging and re-emerging infectious diseases. *Nature* **430**, 242–249 (2004).
- WHO *The World Health Report 2004—Changing History* (2004).
- WHO. Global estimate of the incidence of clinical pneumonia among children under five years of age. *Bull. World Health Organ.* **82**, 891–970 (2004).
- Hohenthal, U. *et al.* Bronchoalveolar lavage in immunocompromised patients with haematological malignancy—value of new microbiological methods. *Eur. J. Haematol.* **74**, 203–211 (2005).
- Sharma, A. & Lokeshwar, N. Febrile neutropenia in haematological malignancies. *J. Postgrad. Med.* **51** (Suppl 1), S42–S48 (2005).
- Shorr, A.F., Susla, G.M. & O'Grady, N.P. Pulmonary infiltrates in the non-HIV-infected immunocompromised patient: etiologies, diagnostic strategies, and outcomes. *Chest* **125**, 260–271 (2004).
- Chang, H.Y. *et al.* Causes of death in adults with acute leukemia. *Medicine (Baltimore)* **55**, 259–268 (1976).
- Whimbey, E., Goodrich, J. & Bodey, G.P. Pneumonia in cancer patients. *Cancer Treat. Res.* **79**, 185–210 (1995).
- Clement, C.G. *et al.* Stimulation of lung innate immunity protects against lethal pneumococcal pneumonia in mice. *Am. J. Respir. Crit. Care Med.* **177**, 1322–1330 (2008).
- Evans, S.E. *et al.* Stimulated innate resistance of lung epithelium protects mice broadly against bacteria and fungi. *Am. J. Respir. Cell Mol. Biol.* **42**, 40–50 (2010).
- Evans, S.E., Xu, Y., Tuvim, M.J. & Dickey, B.F. Inducible innate resistance of lung epithelium to infection. *Annu. Rev. Physiol.* **72**, 413–435 (2010).
- Evans, S.E. *et al.* Inhaled innate immune ligands to prevent pneumonia. *Br. J. Pharmacol.* **163**, 195–206 (2011).
- Safdar, A., Shelburne, S.A., Evans, S.E. & Dickey, B.F. Inhaled therapeutics for prevention and treatment of pneumonia. *Expert Opin. Drug Saf.* **8**, 435–449 (2009).
- Duggan, J.M. *et al.* Synergistic interactions of TLR2/6 and TLR9 induce a high level of resistance to lung infection in mice. *J. Immunol.* **186**, 5916–5926 (2011).
- Tuvim, M.J., Evans, S.E., Clement, C.G., Dickey, B.F. & Gilbert, B.E. Augmented lung inflammation protects against influenza A pneumonia. *PLoS ONE* **4**, e4176 (2009).
- Tuvim, M.J., Gilbert, B.E., Dickey, B.F. & Evans, S.E. Synergistic TLR2/6 and TLR9 activation protects mice against lethal influenza pneumonia. *PLoS ONE* **7**, e30596 (2012).

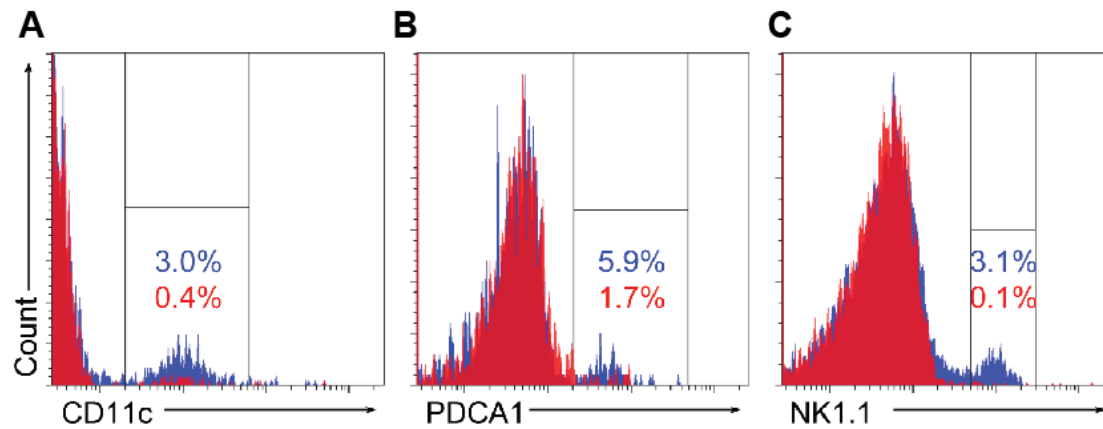
18. Bals, R. & Hiemstra, P.S. Innate immunity in the lung: how epithelial cells fight against respiratory pathogens. *Eur. Respir. J.* **23**, 327–333 (2004).
19. Bartlett, J.A., Fischer, A.J. & McCray, P.B. Jr. Innate immune functions of the airway epithelium. *Contrib. Microbiol.* **15**, 147–163 (2008).
20. Hippenstiel, S., Opitz, B., Schmeck, B. & Suttrop, N. Lung epithelium as a sentinel and effector system in pneumonia—molecular mechanisms of pathogen recognition and signal transduction. *Respir. Res.* **7**, 97 (2006).
21. Mizgerd, J.P. Acute lower respiratory tract infection. *N. Engl. J. Med.* **358**, 716–727 (2008).
22. Schutte, B.C. & McCray, P.B. Jr. β -defensins in lung host defense. *Annu. Rev. Physiol.* **64**, 709–748 (2002).
23. Hammad, H. & Lambrecht, B.N. Dendritic cells and epithelial cells: linking innate and adaptive immunity in asthma. *Nat. Rev. Immunol.* **8**, 193–204 (2008).
24. Strickland, D.H., Upham, J.W. & Holt, P.G. Epithelial-dendritic cell interactions in allergic disorders. *Curr. Opin. Immunol.* **22**, 789–794 (2010).
25. Schreiberl, G. *et al.* Toll-like receptor expression and function in human dendritic cell subsets: implications for dendritic cell-based anti-cancer immunotherapy. *Cancer Immunol. Immunother.* **59**, 1573–1582 (2010).
26. Zaroni, I. & Granucci, F. Regulation of antigen uptake, migration, and lifespan of dendritic cell by Toll-like receptors. *J. Mol. Med. (Berl)* **88**, 873–880 (2010).
27. Seya, T., Kasamatsu, J., Azuma, M., Shime, H. & Matsumoto, M. Natural killer cell activation secondary to innate pattern sensing. *J. Innate Immun.* **3**, 264–273 (2011).
28. Paust, S. & von Andrian, U.H. Natural killer cell memory. *Nat. Immunol.* **12**, 500–508 (2011).
29. Sonnenberg, G.F., Fouser, L.A. & Artis, D. Border patrol: regulation of immunity, inflammation and tissue homeostasis at barrier surfaces by IL-22. *Nat. Immunol.* **12**, 383–390 (2011).
30. Lin, S.C., Lo, Y.C. & Wu, H. Helical assembly in the MyD88-IRAK4-IRAK2 complex in TLR/IL-1R signalling. *Nature* **465**, 885–890 (2010).
31. Wu, H., Lo, Y.C. & Yin, Q. Structural studies of NEMO and TRAF6: implications in NF-kappaB activation. *Adv. Exp. Med. Biol.* **691**, 89–91 (2011).
32. Valkov, E. *et al.* Crystal structure of Toll-like receptor adaptor MAL/TIRAP reveals the molecular basis for signal transduction and disease protection. *Proc. Natl. Acad. Sci. USA* **108**, 14879–14884 (2011).
33. Gay, N.J., Gangloff, M. & O'Neill, L.A. What the Myddosome structure tells us about the initiation of innate immunity. *Trends Immunol.* **32**, 104–109 (2011).
34. Francis, K.P. *et al.* Visualizing pneumococcal infections in the lungs of live mice using bioluminescent *Streptococcus pneumoniae* transformed with a novel gram-positive lux transposon. *Infect. Immun.* **69**, 3350–3358 (2001).
35. Karlstrom, A., Heston, S.M., Boyd, K.L., Tuomanen, E.I. & McCullers, J.A. Toll-like receptor 2 mediates fatal immunopathology in mice during treatment of secondary pneumococcal pneumonia following influenza. *J. Infect. Dis.* **204**, 1358–1366 (2011).
36. Sato, M. *et al.* Multiple oncogenic changes (K-RAS(V12), p53 knockdown, mutant EGFRs, p16 bypass, telomerase) are not sufficient to confer a full malignant phenotype on human bronchial epithelial cells. *Cancer Res.* **66**, 2116–2128 (2006).
37. Naeem, H., Zimmer, R., Tavakkolkhah, P. & Kuffner, R. Rigorous assessment of gene set enrichment tests. *Bioinformatics* **28**, 1480–1486 (2012).
38. Rivals, I., Personnaz, L., Taing, L. & Potier, M.C. Enrichment or depletion of a GO category within a class of genes: which test?. *Bioinformatics* **23**, 401–407 (2007).
39. Agusti, C. *et al.* Inflammatory response associated with pulmonary complications in non-HIV immunocompromised patients. *Thorax* **59**, 1081–1088 (2004).
40. Schleimer, R.P. Glucocorticoids suppress inflammation but spare innate immune responses in airway epithelium. *Proc. Am. Thorac. Soc.* **1**, 222–230 (2004).
41. Bowden, D.H. Cell turnover in the lung. *Am. Rev. Respir. Dis.* **128**, S46–S48 (1983).
42. Rawlins, E.L. & Hogan, B.L. Ciliated epithelial cell lifespan in the mouse trachea and lung. *Am. J. Physiol. Lung Cell. Mol. Physiol.* **295**, L231–L234 (2008).
43. Mijares, L.A. *et al.* Airway epithelial MyD88 restores control of *Pseudomonas aeruginosa* murine infection via an IL-1-dependent pathway. *J. Immunol.* **186**, 7080–7088 (2011).
44. Hatanaka, E., Dermargos, A., Armelin, H.A., Curi, R. & Campa, A. Serum amyloid A induces reactive oxygen species (ROS) production and proliferation of fibroblast. *Clin. Exp. Immunol.* **163**, 362–367 (2011).
45. Ather, J.L. *et al.* Serum amyloid A activates the NLRP3 inflammasome and promotes Th17 allergic asthma in mice. *J. Immunol.* **187**, 64–73 (2011).
46. Shah, C., Hari-Dass, R. & Raynes, J.G. Serum amyloid A is an innate immune opsonin for Gram-negative bacteria. *Blood* **108**, 1751–1757 (2006).
47. Hari-Dass, R., Shah, C., Meyer, D.J. & Raynes, J.G. Serum amyloid A protein binds to outer membrane protein A of gram-negative bacteria. *J. Biol. Chem.* **280**, 18562–18567 (2005).
48. Adachi, O. *et al.* Targeted disruption of the MyD88 gene results in loss of IL-1- and IL-18-mediated function. *Immunity* **9**, 143–150 (1998).
49. Suzuki, N. *et al.* Severe impairment of interleukin-1 and Toll-like receptor signalling in mice lacking IRAK-4. *Nature* **416**, 750–756 (2002).
50. Zheng, Y. *et al.* Interleukin-22, a T(H)17 cytokine, mediates IL-23-induced dermal inflammation and acanthosis. *Nature* **445**, 648–651 (2007).
51. Hou, B., Reizis, B. & DeFranco, A.L. Toll-like receptors activate innate and adaptive immunity by using dendritic cell-intrinsic and -extrinsic mechanisms. *Immunity* **29**, 272–282 (2008).
52. Okubo, T., Knoepfler, P.S., Eisenman, R.N. & Hogan, B.L. Nmyc plays an essential role during lung development as a dosage-sensitive regulator of progenitor cell proliferation and differentiation. *Development* **132**, 1363–1374 (2005).
53. Wyde, P.R., Couch, R.B., Mackler, B.F., Cate, T.R. & Levy, B.M. Effects of low- and high-passage influenza virus infection in normal and nude mice. *Infect. Immun.* **15**, 221–229 (1977).
54. Gilbert, B.E., Wyde, P.R., Ambrose, M.W., Wilson, S.Z. & Knight, V. Further studies with short duration ribavirin aerosol for the treatment of influenza virus infection in mice and respiratory syncytial virus infection in cotton rats. *Antiviral Res.* **17**, 33–42 (1992).
55. Clement, C.G. *et al.* Allergic lung inflammation alters neither susceptibility to *Streptococcus pneumoniae* infection nor inducibility of innate resistance in mice. *Respir. Res.* **10**, 70 (2009).
56. You, Y., Richer, E.J., Huang, T. & Brody, S.L. Growth and differentiation of mouse tracheal epithelial cells: selection of a proliferative population. *Am. J. Physiol. Lung Cell. Mol. Physiol.* **283**, L1315–L1321 (2002).

Supplemental Figure 1.



Depletion of neutrophils with anti-Ly6G antibody. (A) Quantification of BAL neutrophils by cytology. Mice were depleted of neutrophils with 100 μ g anti-Ly6G Ab intraperitoneally prior to aerosolized treatment with Pam2-ODN or PBS (sham). 24 h after the aerosolized treatment, the mice were submitted to BAL, and the centrifuged samples were Wright-Giemsa stained. Shown are the differential percentages of neutrophils in BAL fluid of 300 counted cells. (N.D.: none detected) (B) Quantification of lung neutrophils by flow-cytometry. Representative results obtained from cells dispersed from lung and labeled with Gr1-APC antibody. Lungs were harvested from a naïve mouse (baseline, left panels) or from mice challenged with *Pseudomonas* without (infected, middle panels) or with (infected and depleted, right panels) neutrophil depletion. The box in the scattergrams (top panels) represent the predicted forward and side scatters of mouse granulocytes. Cells labeled by Gr1-APC (bottom panels) are presented in red. The indicated percentages represent the proportion of all lung cells that met the forward scatter, side scatter and antibody-binding criteria for neutrophils in each sample.

Supplemental Figure 2



Leukocyte flow cytometry. (A) Mice expressing the diphtheria toxin receptor under the *CD11c* promoter (*CD11c*-DTR) were treated with intratracheal diphtheria toxin or PBS. Shown is flow cytometry of disaggregated whole lungs for CD11c positive cells from sham (blue) or toxin (red) treated mice. (B) Flow cytometry of disaggregated lungs for PDCA1-positive cells for mice treated with depleting anti-PDCA Ab (red) or PBS (blue). (C) Flow cytometry of disaggregated lungs for NK1.1-positive cells for mice treated with depleting anti-NK1.1 Ab (red) or PBS (blue).

Supplemental Table 1. Differentially expressed genes shown in Figure 6. mRNA was harvested from C56BL/6 mouse lung homogenates (“Lung”) or from MLE-15 cells (“Cell”) 4 h after treatment with Pam2-ODN or PBS, then submitted to microarray analysis. Shown are fold change transcript levels comparing PBS-treated samples to Pam2-ODN-treated samples for the designated sample type. Tukey honestly significant difference (HSD) test was used to compare the differences between each pair of means with appropriate adjustments for multiple testing. A false discovery rate of <0.05 was used, and p value comparing means of PBS-treated to Pam2-ODN-treated samples was <0.0006 for all reported transcripts.

Probe	Lung Fold Change	Cell Fold Change	Transcript
<i>AADACL1</i>	-1.31	-1.47	Arylacetamide deacetylase-like 1
<i>AATK</i>	-1.32	-1.34	Apoptosis-associated tyrosine kinase
<i>ABCB1B</i>	2.86	1.70	ATP-binding cassette, sub-family B (MDR/TAP), member 1B
<i>ABHD14B</i>	-1.44	-1.51	Abhydrolase domain containing 14b
<i>ABR</i>	1.36	1.65	Active BCR-related gene
<i>ABTB1</i>	-2.22	-1.49	Ankyrin repeat and BTB (POZ) domain containing 1
<i>ACAD9</i>	1.64	1.21	Acyl-Coenzyme A dehydrogenase family, member 9
<i>ACADS</i>	-1.87	-1.72	Acyl-Coenzyme A dehydrogenase, short chain
<i>ACADSB</i>	-1.69	-1.35	Acyl-Coenzyme A dehydrogenase, short/branched chain
<i>ACOT1</i>	-1.47	-1.88	Acyl-CoA thioesterase 1
<i>ACPL2</i>	-1.75	-1.42	Acid phosphatase-like 2
<i>ADCK4</i>	-1.80	-1.96	aarF domain containing kinase 4
<i>ADSSL1</i>	-1.31	-1.21	Adenylosuccinate synthetase like 1
<i>AGGF1</i>	1.28	1.16	Angiogenic factor with G patch and FHA domains 1
<i>AI449175</i>	1.60	1.20	Expressed sequence AI449175
<i>AI467606</i>	-1.53	-1.27	Expressed sequence AI467606
<i>AI894139</i>	-1.63	-1.62	Expressed sequence AI894139
<i>AIFM2</i>	-1.71	-1.33	Apoptosis-inducing factor, mitochondrion-associated 2
<i>AIP</i>	-1.30	-1.26	Aryl-hydrocarbon receptor-interacting protein
<i>AKAP8L</i>	-2.02	-1.51	A kinase anchor protein 8-like
<i>ALDH3B1</i>	-1.32	-1.42	Aldehyde dehydrogenase 3 family, member B1
<i>ALDOC</i>	-1.76	-1.36	Aldolase 3, C isoform
<i>ALKBH7</i>	-2.33	-1.48	AlkB, alkylation repair homolog 7
<i>ANAPC13</i>	-1.30	-1.26	Anaphase promoting complex subunit 13
<i>ANGPTL2</i>	-1.29	-1.45	Angiopietin-like 2
<i>ANKS6</i>	-1.37	-2.13	Ankyrin repeat and sterile alpha motif domain containing 6
<i>ANXA3</i>	1.21	1.21	Annexin A3
<i>APOA1BP</i>	-1.20	-1.40	Apolipoprotein A-I binding protein
<i>APPL2</i>	-1.19	-1.28	Adaptor protein, phosphotyrosine interaction, PH domain and leucine zipper containing 2
<i>ARD1</i>	-1.36	-1.12	N-acetyltransferase ARD1 homolog
<i>ARG2</i>	3.54	1.91	arginase type II
<i>ARHGEF19</i>	-2.39	-2.28	Rho guanine nucleotide exchange factor 19
<i>ATAD1</i>	1.31	1.45	ATPase family, AAA domain containing 1
<i>ATE1</i>	-1.37	-1.16	Arginine-tRNA-protein transferase 1
<i>ATF7IP</i>	-1.30	-1.35	Activating transcription factor 7 interacting protein
<i>ATOX1</i>	-3.22	-1.25	Antioxidant protein 1 homolog 1
<i>ATP1B3</i>	1.33	1.16	ATPase, Na ⁺ /K ⁺ transporting, beta 3 polypeptide

<i>AU019823</i>	2.33	1.71	Expressed sequence AU019823
<i>AU040829</i>	1.37	1.24	Expressed sequence AU040829
<i>AZI1</i>	-1.38	-1.71	5-azacytidine induced gene 1
<i>B3GNT1</i>	-1.24	-1.41	UDP-GlcNAc:betaGal beta-1,3-N-acetylglucosaminyltransferase 1
<i>B3GNT8</i>	-2.30	-2.39	UDP-GlcNAc:betaGal beta-1,3-N-acetylglucosaminyltransferase 8
<i>B9D1</i>	-1.40	-1.36	B9 protein domain 1
<i>BACH2</i>	2.20	1.22	BTB and CNC homology 2
<i>BAG4</i>	1.39	1.14	BCL2-associated athanogene 4
<i>BBS7</i>	-1.22	-1.67	Bardet-Biedl syndrome 7
<i>BC004044</i>	1.57	1.45	cDNA sequence BC004044
<i>BC008155</i>	-1.35	-1.39	cDNA sequence BC008155
<i>BC053749</i>	-1.57	-1.51	cDNA sequence BC053749
<i>BCAR1</i>	2.25	1.44	Breast cancer anti-estrogen resistance 1
<i>BCAS1</i>	-1.35	-1.14	Breast carcinoma amplified sequence 1
<i>BCL10</i>	1.37	1.77	B-cell leukemia/lymphoma 10
<i>BCL2A1C</i>	5.04	3.14	B-cell leukemia/lymphoma 2 related protein A1c
<i>BCL2A1D</i>	8.17	4.78	B-cell leukemia/lymphoma 2 related protein A1d
<i>BCL2L2</i>	1.57	1.16	Bcl2-like 2
<i>BCL3</i>	7.04	4.38	B-cell leukemia/lymphoma 3
<i>BID</i>	1.35	2.27	BH3 interacting domain death agonist
<i>BIRC2</i>	1.16	1.36	Baculoviral IAP repeat-containing 2
<i>BMP6</i>	1.34	2.13	Bone morphogenetic protein 6
<i>BOLA1</i>	-2.33	-1.26	BolA-like 1
<i>BRWD1</i>	1.31	1.25	Bromodomain and WD repeat domain containing 1
<i>BTG1</i>	1.16	1.21	B-cell translocation gene 1, anti-proliferative
<i>BZW2</i>	1.22	1.12	Basic leucine zipper and W2 domains 2
<i>C80913</i>	2.06	1.42	Expressed sequence C80913)
<i>CALCB</i>	1.43	2.89	Calcitonin-related polypeptide, beta
<i>CAMK2D</i>	2.30	1.27	Calcium/calmodulin-dependent protein kinase II, delta
<i>CARM1</i>	1.90	1.72	Coactivator-associated arginine methyltransferase 1
<i>CASP1</i>	1.73	1.94	Caspase 1
<i>CASP4</i>	3.67	5.34	Caspase 4, apoptosis-related cysteine peptidase
<i>CASP9</i>	-1.21	-1.39	Caspase 9
<i>CC2D2A</i>	-1.43	-1.50	Coiled-coil and C2 domain containing 2A
<i>CCDC111</i>	-1.35	-1.60	Coiled-coil domain containing 111
<i>CCDC43</i>	1.33	1.23	Coiled-coil domain containing 43
<i>CCDC86</i>	1.68	1.28	Coiled-coil domain containing 86
<i>CCL5</i>	1.47	4.84	Chemokine (C-C motif) ligand 5
<i>CCND2</i>	1.33	1.37	Cyclin D2
<i>CCRN4L</i>	1.29	1.43	CCR4 carbon catabolite repression 4-like
<i>CD14</i>	4.24	1.96	CD14 antigen

<i>CD74</i>	2.17	9.92	CD74 antigen
<i>CD81</i>	-1.19	-1.14	CD 81 antigen
<i>CD83</i>	5.20	3.47	CD83 antigen
<i>CDC16</i>	1.44	1.28	CDC16 cell division cycle 16 homolog
<i>CEBPB</i>	1.75	1.94	CCAAT/enhancer binding protein, beta
<i>CEP164</i>	-1.43	-1.58	Centrosomal protein 164, transcript variant 1
<i>CHCHD5</i>	-1.53	-1.30	Coiled-coil-helix-coiled-coil-helix domain containing 5
<i>CHCHD8</i>	-1.39	-1.34	Coiled-coil-helix-coiled-coil-helix domain containing 8
<i>CHI3L1</i>	1.61	5.16	Chitinase 3-like 1
<i>CHKB</i>	-1.30	-1.48	Choline kinase beta
<i>CIB2</i>	-1.25	-1.41	Calcium and integrin binding family member 2
<i>CIRBP</i>	-1.51	-1.86	Cold inducible RNA binding protein
<i>CISH</i>	2.78	2.92	Cytokine inducible SH2-containing protein
<i>CKMT1</i>	-2.15	-1.40	Creatine kinase, mitochondrial 1, ubiquitous
<i>CLIP4</i>	2.94	1.29	CAP-GLY domain containing linker protein family, member 4
<i>CLTA</i>	-1.50	-1.19	Clathrin, light polypeptide
<i>CML1</i>	-1.20	-1.77	Camello-like 1
<i>COMMD6</i>	-1.39	-1.25	COMM domain containing 6
<i>COPE</i>	-1.77	-1.27	Coatomer protein complex, subunit epsilon
<i>COQ6</i>	-1.50	-1.21	Coenzyme Q6 homolog
<i>CORO1B</i>	-1.60	-1.20	Coronin, actin binding protein 1B
<i>CPNE2</i>	-1.57	-1.28	Copine II
<i>CSDE1</i>	1.65	1.19	Cold shock domain containing E1, RNA binding
<i>CSF1</i>	3.83	4.85	Colony stimulating factor 1 (macrophage)
<i>CSRP2</i>	-1.56	-1.36	Cysteine and glycine-rich protein 2
<i>CSTF1</i>	-1.57	-1.20	Cleavage stimulation factor, 3' pre-RNA, subunit 1
<i>CTPS</i>	3.66	1.28	Cytidine 5'-triphosphate synthase
<i>CTSC</i>	1.38	1.82	Cathepsin C
<i>CTTNBP2NL</i>	1.25	1.30	CTTNBP2 N-terminal like
<i>CUL4A</i>	1.30	1.23	Cullin 4A
<i>CX3CL1</i>	2.39	4.54	Chemokine (C-X3-C motif) ligand 1
<i>CXADR</i>	1.74	1.33	Coxsackievirus and adenovirus receptor
<i>CXCL1</i>	20.03	90.91	Chemokine (C-X-C motif) ligand 1
<i>CXCL10</i>	42.27	6.90	Chemokine (C-X-C motif) ligand 10
<i>CXCL16</i>	1.33	2.64	Chemokine (C-X-C motif) ligand 16
<i>CXCL2</i>	28.54	36.68	Chemokine (C-X-C motif) ligand 2
<i>CYP2S1</i>	-1.37	-1.92	Cytochrome P450, family 2, subfamily s, polypeptide 1
<i>CYP4F16</i>	-1.60	-1.48	Cytochrome P450, family 4, subfamily f, polypeptide 16
<i>D0H4S114</i>	-1.46	-1.66	DNA segment, human D4S114
<i>D10JHU81E</i>	-1.26	-1.42	DNA segment, Chr 10, Johns Hopkins University 81 expressed
<i>D19ERTD721E</i>	-1.35	-1.14	DNA segment, Chr 19, ERATO Doi 721, expressed

<i>D9ERTD392E</i>	-1.44	-1.38	Cell cycle progression gene 1
<i>DBP</i>	-1.43	-2.05	D site albumin promoter binding protein
<i>DCXR</i>	-1.19	-1.31	Dicarbonyl L-xylulose reductase
<i>DEB1</i>	-1.33	-1.21	Differentially expressed in B16F10 1
<i>DENR</i>	1.58	1.34	Density-regulated protein
<i>DGCR6</i>	-1.90	-1.44	DiGeorge syndrome critical region gene 6
<i>DLG3</i>	-1.34	-1.48	Discs, large homolog 3 (Drosophila)
<i>DMN</i>	1.58	1.59	Desmuslin
<i>DNAJB10</i>	-1.62	-1.40	DnaJ (Hsp40) homolog, subfamily B, member 10
<i>DNAJC16</i>	-1.18	-1.26	DnaJ (Hsp40) homolog, subfamily C, member 16
<i>DNM1L</i>	1.40	1.32	Dynamin 1-like
<i>DOK3</i>	-1.52	-2.30	Docking protein 3
<i>DPM2</i>	-1.30	-1.20	Dolichol-phosphate (beta-D) mannosyltransferase 2
<i>DPM3</i>	-1.49	-1.32	Dolichyl-phosphate mannosyltransferase polypeptide 3
<i>DPP4</i>	-1.14	-2.32	Dipeptidylpeptidase 4
<i>DPP7</i>	-1.47	-1.27	Dipeptidylpeptidase 7
<i>DPY30</i>	-1.71	-1.13	Dpy-30 homolog
<i>DTX2</i>	-1.19	-1.26	Deltex 2 homolog
<i>DUSP16</i>	1.41	1.70	Dual specificity phosphatase 16
<i>DUSP8</i>	1.50	1.95	Dual specificity phosphatase 8
<i>DYM</i>	-1.24	-1.42	Dymeclin
<i>DYRK3</i>	1.60	1.38	Dual-specificity tyrosine-(Y)-phosphorylation regulated kinase 3
<i>E2F2</i>	1.76	1.52	E2F transcription factor 2
<i>EBPL</i>	-1.23	-1.58	Emopamil binding protein-like
<i>ECE1</i>	-1.53	-1.40	Endothelin converting enzyme 1
<i>ECH1</i>	-1.15	-1.39	Enoyl coenzyme A hydratase 1, peroxisomal
<i>EFCAB4A</i>	-1.29	-1.68	EF-hand calcium binding domain 4A
<i>EIF1A</i>	1.35	1.29	Eukaryotic translation initiation factor 1A
<i>EIF4A1</i>	1.28	1.17	Eukaryotic translation initiation factor 4A1
<i>ELA1</i>	-1.79	-1.61	Elastase 1
<i>ELF3</i>	1.50	1.48	E74-like factor 3
<i>ELOF1</i>	-1.37	-1.24	Elongation factor 1 homolog
<i>ENO3</i>	-2.08	-1.24	Enolase 3, beta muscle
<i>ENPP2</i>	1.54	1.93	Ectonucleotide pyrophosphatase/phosphodiesterase 2
<i>EPHX1</i>	-1.16	-1.45	Epoxide hydrolase 1, microsomal
<i>EPS8L2</i>	-1.21	-1.43	EPS8-like 2
<i>ERP29</i>	-1.98	-1.22	Endoplasmic reticulum protein 29
<i>ETFB</i>	-1.93	-1.22	Electron transferring flavoprotein, beta polypeptide
<i>ETHE1</i>	-1.26	-1.29	Ethylmalonic encephalopathy 1
<i>ETS2</i>	1.35	1.32	E26 avian leukemia oncogene 2, 3' domain
<i>EVI5L</i>	-1.50	-2.11	Ecotropic viral integration site 5 like

<i>EXOSC1</i>	1.48	1.35	Exosome component 1
<i>EXT1</i>	1.42	1.45	Exostoses (multiple)
<i>EXTL2</i>	1.17	1.16	Exostoses (multiple)-like 2
<i>EXTL3</i>	-1.27	-1.21	Exostoses (multiple)-like 3
<i>FAAH</i>	-1.73	-1.34	Fatty acid amide hydrolase
<i>FADS1</i>	-1.18	-1.22	Fatty acid desaturase 1
<i>FARS2</i>	-1.27	-1.37	Phenylalanine-tRNA synthetase 2
<i>FAS</i>	2.76	2.86	Fas (TNF receptor superfamily member 6)
<i>FBXO18</i>	-1.42	-1.44	F-box protein 18
<i>FBXO36</i>	-1.90	-1.60	F-box protein 36
<i>FBXO44</i>	-1.39	-1.45	F-box protein 44
<i>FCHO1</i>	-1.59	-1.36	FCH domain only 1
<i>FDXR</i>	-1.75	-1.67	Ferredoxin reductase
<i>FEN1</i>	1.37	1.14	Flap structure specific endonuclease 1
<i>FGF13</i>	1.34	2.35	Fibroblast growth factor 13
<i>FHL1</i>	-1.19	-1.50	Four and a half LIM domains 1
<i>FLCN</i>	-1.22	-1.35	Folliculin
<i>FLOT1</i>	-1.86	-1.29	Flotillin 1
<i>FNDC3B</i>	1.86	2.15	Fibronectin type III domain containing 3B
<i>FXC1</i>	-1.25	-1.27	Fractured callus expressed transcript 1
<i>FXYD5</i>	-1.21	-1.26	FXYD domain-containing ion transport regulator 5
<i>G0S2</i>	-1.53	-1.95	G0/G1 switch gene 2
<i>G3BP1</i>	1.44	1.52	Ras-GTPase-activating protein SH3-domain binding protein 1
<i>GALK1</i>	-1.47	-1.25	Galactokinase 1
<i>GALT</i>	-1.40	-1.44	Galactose-1-phosphate uridyl transferase
<i>GAMT</i>	-1.52	-1.97	Guanidinoacetate methyltransferase
<i>GANC</i>	-1.39	-1.43	Glucosidase, alpha; neutral C
<i>GBP2</i>	2.22	2.18	Guanylate nucleotide binding protein 2
<i>GBP3</i>	1.79	2.17	Guanylate nucleotide binding protein 3
<i>GCDH</i>	-1.63	-1.37	Glutaryl-Coenzyme A dehydrogenase
<i>GDPD1</i>	-1.45	-1.22	Glycerophosphodiester phosphodiesterase domain containing 1
<i>GDPD5</i>	2.26	2.10	Glycerophosphodiester phosphodiesterase domain containing 5
<i>GFPT2</i>	2.86	1.91	Glutamine fructose-6-phosphate transaminase 2
<i>GLB1</i>	-1.38	-1.34	Galactosidase, beta 1
<i>GLIPR2</i>	1.61	2.08	GLI pathogenesis-related 2
<i>GLIS2</i>	2.25	2.20	GLIS family zinc finger 2
<i>GM114</i>	-1.36	-1.38	Gene model 114
<i>GMFG</i>	-1.48	-1.27	Glia maturation factor, gamma
<i>GNAQ</i>	1.48	1.40	Guanine nucleotide binding protein, alpha q polypeptide
<i>GNA-RS1</i>	1.83	1.35	Guanine nucleotide binding protein, related sequence 1
<i>GNL3</i>	1.24	1.40	Guanine nucleotide binding protein-like 3

<i>GOLGA2</i>	-1.31	-1.21	Golgi autoantigen, golgin subfamily a, 2
<i>GORASP1</i>	-1.26	-1.60	Golgi reassembly stacking protein 1
<i>GPR109A</i>	3.80	5.02	G protein-coupled receptor 109A
<i>GPR146</i>	-1.19	-1.64	G protein-coupled receptor 146
<i>GPS2</i>	-1.62	-1.13	G protein pathway suppressor 2
<i>GPT2</i>	-2.31	-1.45	Glutamic pyruvate transaminase (alanine aminotransferase) 2
<i>GRB7</i>	-1.74	-1.21	Growth factor receptor bound protein 7
<i>GRHL2</i>	1.44	1.85	Grainyhead-like 2
<i>GRHPR</i>	-1.71	-1.63	Glyoxylate reductase/hydroxypyruvate reductase
<i>GRTP1</i>	-2.11	-1.79	GH regulated TBC protein 1
<i>GSPT1</i>	1.34	1.19	G1 to S phase transition 1
<i>GSTM1</i>	-1.55	-1.31	Glutathione S-transferase, mu 1
<i>GSTZ1</i>	-1.69	-1.20	Glutathione transferase zeta 1
<i>GTPBP4</i>	1.30	1.27	GTP binding protein 4
<i>H2-DMB1</i>	-1.44	-1.74	Histocompatibility 2, class II, locus Mb1
<i>HAGHL</i>	-1.66	-1.49	Hydroxyacylglutathione hydrolase-like
<i>HAP1</i>	-1.36	-1.32	Huntingtin-associated protein 1
<i>HDGFRP2</i>	-1.28	-1.22	Hepatoma-derived growth factor, related protein 2
<i>HEBP1</i>	-1.38	-1.27	Heme binding protein 1
<i>HELB</i>	-1.37	-1.24	Helicase B
<i>HIST2H2AB</i>	-1.93	-1.45	Histone cluster 2, H2ab
<i>HIST2H2BE</i>	-1.38	-1.71	Histone cluster 2, H2be
<i>HN1L</i>	2.12	1.72	Hematological and neurological expressed 1-like
<i>HPX</i>	2.00	2.32	Hemopexin
<i>HS6ST1</i>	1.89	1.92	Heparan sulfate 6-O-sulfotransferase
<i>HSD17B10</i>	-1.76	-1.30	Hydroxysteroid (17-beta) dehydrogenase 10
<i>HSD3B7</i>	-1.16	-1.38	Hydroxy-delta-5-steroid dehydrogenase, 3 beta- and steroid delta-isomerase 7
<i>HSF1</i>	1.28	1.19	Heat shock factor 1
<i>ICAM1</i>	3.15	1.81	Intercellular adhesion molecule 1
<i>ICT1</i>	-1.57	-1.43	Immature colon carcinoma transcript 1
<i>IFI47</i>	2.57	6.80	Interferon gamma inducible protein 47
<i>IFITM3</i>	1.31	1.27	Interferon induced transmembrane protein 3
<i>IFNGR1</i>	1.38	1.57	Interferon gamma receptor 1
<i>IFT172</i>	-1.67	-1.29	Intraflagellar transport 172 homolog
<i>IGF2R</i>	-1.47	-1.27	Insulin-like growth factor 2 receptor
<i>IL11RA1</i>	-1.76	-1.38	Interleukin 11 receptor, alpha chain 1
<i>IL33</i>	3.75	1.76	Interleukin 33
<i>IL6</i>	3.60	3.86	Interleukin 6
<i>INPP5E</i>	-1.36	-1.19	Inositol polyphosphate-5-phosphatase E
<i>IRF1</i>	1.51	1.91	Interferon regulatory factor 1
<i>IRF5</i>	1.50	2.93	Interferon regulatory factor 5

<i>ITGAV</i>	1.61	1.71	Integrin alpha V
<i>ITGB4</i>	-1.79	-1.33	Integrin beta 4
<i>ITGB6</i>	1.70	2.22	Integrin beta 6
<i>ITIH2</i>	-1.88	-1.41	Inter-alpha trypsin inhibitor, heavy chain 2
<i>JAK2</i>	2.18	1.55	Janus kinase 2
<i>JMJD3</i>	1.34	1.32	Jumonji domain containing 3
<i>KCTD2</i>	-1.29	-1.29	Potassium channel tetramerisation domain containing 2
<i>KHK</i>	-1.57	-1.30	Ketohexokinase
<i>KLK10</i>	1.56	1.27	Kallikrein related-peptidase 10
<i>LCN2</i>	3.28	4.66	Lipocalin 2
<i>LDB1</i>	-1.19	-1.23	LIM domain binding 1
<i>LGALS4</i>	-1.36	-1.15	Lectin, galactose binding, soluble 4
<i>LIF</i>	1.33	4.62	Leukemia inhibitory factor
<i>LIMK2</i>	-1.15	-1.25	LIM motif-containing protein kinase 2
<i>LIN54</i>	1.46	1.32	Lin-54 homolog
<i>LITAF</i>	2.02	1.27	LPS-induced TN factor
<i>LMAN2L</i>	-1.43	-1.33	Lectin, mannose-binding 2-like
<i>LRP12</i>	1.47	1.38	Low density lipoprotein-related protein 12
<i>LRRC49</i>	-1.57	-1.42	Leucine rich repeat containing 49
<i>LRRC8D</i>	1.37	1.37	Leucine rich repeat containing 8D
<i>LRSAM1</i>	-1.75	-1.47	Leucine rich repeat and sterile alpha motif containing 1
<i>LTV1</i>	1.41	1.41	LTV1 homolog
<i>LY6G6C</i>	-2.65	-1.36	Lymphocyte antigen 6 complex, locus G6C
<i>LYAR</i>	1.50	1.34	Ly1 antibody reactive clone
<i>LYPD2</i>	-1.67	-1.39	Ly6/Plaur domain containing 2
<i>MAD2L1BP</i>	-1.45	-1.27	MAD2L1 binding protein
<i>MAP3K7IP1</i>	-1.33	-1.38	Mitogen-activated protein kinase kinase kinase 7 interacting protein 1
<i>MAP3K8</i>	2.67	5.15	Mitogen-activated protein kinase kinase kinase 8
<i>MAPK6</i>	2.15	1.48	Mitogen-activated protein kinase 6
<i>MBNL2</i>	1.43	1.22	Muscleblind-like 2
<i>MCEE</i>	-1.36	-1.36	Methylmalonyl CoA epimerase
<i>MCF2L</i>	-1.49	-1.59	Mcf.2 transforming sequence-like
<i>METAP1</i>	1.33	1.18	Methionyl aminopeptidase 1
<i>MFSD3</i>	-1.57	-1.41	Major facilitator superfamily domain containing 3
<i>MGAT4B</i>	1.85	1.27	Mannoside acetylglucosaminyltransferase 4, isoenzyme B
<i>MGST2</i>	-2.64	-1.52	Microsomal glutathione S-transferase 2
<i>MKLN1</i>	-1.35	-1.30	Muskelin 1, intracellular mediator containing kelch motifs
<i>MMP13</i>	2.49	1.60	Matrix metalloproteinase 13
<i>MNS1</i>	-1.54	-1.39	Meiosis-specific nuclear structural protein 1
<i>MOBK2C</i>	1.65	1.66	MOB1, Mps One Binder kinase activator-like 2C
<i>MRPL2</i>	-3.13	-1.50	Mitochondrial ribosomal protein L2

<i>MRPL4</i>	1.56	1.59	Mitochondrial ribosomal protein L4
<i>MRPS28</i>	-1.37	-1.17	Mitochondrial ribosomal protein S28
<i>MRPS9</i>	-1.40	-1.23	Mitochondrial ribosomal protein S9
<i>MSH2</i>	-1.82	-1.47	MutS homolog 2
<i>MTAP</i>	1.30	1.27	Methylthioadenosine phosphorylase
<i>MTMR14</i>	1.32	1.13	Myotubularin related protein 14
<i>MUC1</i>	1.53	1.34	Mucin 1, transmembrane
<i>MUTED</i>	-1.21	-1.26	Muted
<i>MXRA7</i>	-1.53	-1.40	Matrix-remodelling associated 7
<i>MYD88</i>	1.78	1.64	Myeloid differentiation primary response gene 88
<i>MYH6</i>	-14.01	-2.10	Myosin, heavy polypeptide 6, cardiac muscle, alpha
<i>MYST4</i>	-1.39	-1.31	MYST histone acetyltransferase monocytic leukemia 4
<i>N4BP2</i>	1.99	1.30	NEDD4 binding protein 2
<i>N6AMT2</i>	-2.48	-1.28	N-6 adenine-specific DNA methyltransferase 2
<i>NAB1</i>	1.28	1.73	Ngfi-A binding protein 1
<i>NDUFA13</i>	-1.16	-1.16	NADH dehydrogenase (ubiquinone) 1 alpha subcomplex, 13
<i>NDUFB8</i>	-1.31	-1.18	NADH dehydrogenase (ubiquinone) 1 beta subcomplex 8
<i>NFKB1</i>	1.99	4.35	Nuclear factor of kappa light polypeptide gene enhancer in B-cells 1, p105
<i>NFKB2</i>	3.01	3.20	Nuclear factor of kappa light polypeptide gene enhancer in B-cells 2 (p49/p100)
<i>NFKBIA</i>	4.62	11.17	Nuclear factor of kappa light polypeptide gene enhancer in B-cells inhibitor, alpha
<i>NFKBID</i>	2.17	3.08	Nuclear factor of kappa light polypeptide gene enhancer in B-cells inhibitor, delta
<i>NFKBIE</i>	8.35	3.39	Nuclear factor of kappa light polypeptide gene enhancer in B-cells inhibitor, epsilon
<i>NFKBIZ</i>	2.64	32.48	Nuclear factor of kappa light polypeptide gene enhancer in B-cells inhibitor, zeta
<i>NME3</i>	-1.23	-1.42	Non-metastatic cells 3, protein expressed in
<i>NMRAL1</i>	-1.59	-1.25	NmrA-like family domain containing 1
<i>NOL1</i>	1.50	1.43	Nucleolar protein 1
<i>NOL5</i>	1.46	1.42	Nucleolar protein 5
<i>NPHP1</i>	-1.59	-1.46	Nephronophthisis 1 (juvenile) homolog
<i>NRM</i>	-1.62	-1.36	Nurim
<i>NSUN4</i>	-1.17	-1.34	NOL1/NOP2/Sun domain family, member 4
<i>NT5M</i>	-1.22	-1.28	5',3'-nucleotidase, mitochondrial
<i>NTHL1</i>	-2.12	-1.57	Nth (endonuclease III)-like 1
<i>NUDT1</i>	-1.57	-1.39	Nudix (nucleoside diphosphate linked moiety X)-type motif 1
<i>NUP98</i>	2.03	1.48	Nucleoporin 98
<i>OAZ2</i>	-1.37	-1.48	Ornithine decarboxylase antizyme 2
<i>OMA1</i>	-1.11	-1.30	OMA1 homolog, zinc metallopeptidase
<i>OSMR</i>	2.91	2.32	Oncostatin M receptor
<i>PA2G4</i>	1.62	1.50	Proliferation-associated 2G4

<i>PAOX</i>	-1.41	-1.32	Polyamine oxidase
<i>PARK7</i>	-1.13	-1.30	Parkinson disease (autosomal recessive, early onset) 7
<i>PARP1</i>	-1.24	-1.15	Poly (ADP-ribose) polymerase family, member 1
<i>PARP14</i>	1.62	1.62	Poly (ADP-ribose) polymerase family, member 14
<i>PARP8</i>	2.31	2.27	Poly (ADP-ribose) polymerase family, member 8
<i>PBX2</i>	-1.48	-1.43	Pre B-cell leukemia transcription factor 2
<i>PCGF6</i>	1.78	1.40	Polycomb group ring finger 6
<i>PCNT</i>	-1.39	-1.56	Pericentrin
<i>PDCD10</i>	1.64	1.27	Programmed cell death 10
<i>PDGFA</i>	1.28	1.60	Platelet-derived growth factor alpha
<i>PDIK1L</i>	2.60	1.38	PDLIM1 interacting kinase 1 like
<i>PDLIM1</i>	-1.25	-1.23	PDZ and LIM domain 1
<i>PDSS1</i>	2.04	1.42	Prenyl diphosphate synthase, subunit 1
<i>PELI1</i>	1.55	1.50	Pellino 1
<i>PER2</i>	1.16	1.15	Period homolog 2
<i>PEX6</i>	-1.30	-1.31	Peroxisomal biogenesis factor 6
<i>PHLDA1</i>	2.35	1.77	Pleckstrin homology-like domain, family A, member 1
<i>PIH1D1</i>	-1.32	-1.33	PIH1 domain containing 1
<i>PITPNC1</i>	1.69	2.43	Phosphatidylinositol transfer protein, cytoplasmic 1
<i>PKP2</i>	1.33	1.17	Plakophilin 2
<i>PLLP</i>	-1.28	-1.45	Plasma membrane proteolipid
<i>PMVK</i>	-1.47	-1.40	Phosphomevalonate kinase
<i>PNO1</i>	1.57	1.35	Partner of NOB1 homolog
<i>PON3</i>	-1.45	-1.31	Paraoxonase 3
<i>POR</i>	-1.39	-1.78	P450 (cytochrome) oxidoreductase
<i>PPFIBP2</i>	-1.36	-1.76	Protein tyrosine phosphatase, receptor-type, F interacting protein, binding protein 2
<i>PPP1R2</i>	1.46	1.23	Protein phosphatase 1, regulatory subunit 2
<i>PPP3CA</i>	1.30	1.20	Protein phosphatase 3, catalytic subunit, alpha isoform
<i>PPP4R1</i>	1.27	1.16	Protein phosphatase 4, regulatory subunit 1
<i>PPS</i>	-1.16	-1.33	Putative phosphatase
<i>PQLC1</i>	1.28	1.16	PQ loop repeat containing 1
<i>PREI4</i>	1.65	1.58	Preimplantation protein 4
<i>PRKCZ</i>	-1.31	-1.61	Protein kinase C, zeta
<i>PRR7</i>	3.27	2.95	Proline rich 7
<i>PRSS8</i>	-1.80	-1.41	Protease, serine, 8
<i>PSMG3</i>	-1.57	-1.24	proteasome (prosome, macropain) assembly chaperone 3
<i>PTDSS2</i>	-1.44	-1.29	Phosphatidylserine synthase 2
<i>PTS</i>	-1.30	-1.25	6-pyruvoyl-tetrahydropterin synthase
<i>PXMP4</i>	-1.81	-1.69	Peroxisomal membrane protein 4
<i>RAB14</i>	-1.36	-1.20	RAB14, member RAS oncogene family
<i>RAG1AP1</i>	-1.17	-1.33	Recombination activating gene 1 activating protein 1

<i>RAI14</i>	1.47	1.50	Retinoic acid induced 14
<i>RAMP1</i>	-1.74	-1.88	Receptor activity modifying protein 1
<i>RASA2</i>	2.01	1.70	RAS p21 protein activator 2
<i>RAVER1</i>	1.99	1.54	Ribonucleoprotein, PTB-binding 1
<i>RBM4B</i>	-1.33	-1.23	RNA binding motif protein 4B
<i>RBM5</i>	-1.23	-1.22	RNA binding motif protein 5
<i>RBMS1</i>	1.47	1.64	RNA binding motif, single stranded interacting protein 1
<i>RCL1</i>	2.04	1.63	RNA terminal phosphate cyclase-like 1
<i>REL</i>	1.90	2.37	Reticuloendotheliosis oncogene
<i>RELA</i>	1.17	1.16	v-rel reticuloendotheliosis viral oncogene homolog A (avian)
<i>RELB</i>	4.18	7.46	Avian reticuloendotheliosis viral (v-rel) oncogene related B
<i>RENBP</i>	-1.71	-1.29	Renin binding protein
<i>RETSAT</i>	-1.90	-1.36	Retinol saturase
<i>REV3L</i>	1.51	1.48	REV3-like, catalytic subunit of DNA polymerase zeta RAD54 like
<i>RFC2</i>	-1.88	-1.20	Replication factor C (activator 1) 2
<i>RFC5</i>	-2.20	-1.30	Replication factor C (activator 1) 5
<i>RGS16</i>	4.31	1.71	Regulator of G-protein signaling 16
<i>RGS4</i>	1.58	6.22	Regulator of G-protein signaling 4
<i>RHBDL3</i>	2.87	2.12	Rhomboid, veinlet-like 3
<i>RHOF</i>	3.66	2.03	Ras homolog gene family, member f
<i>RHOU</i>	2.30	1.70	Ras homolog gene family, member U
<i>RIPK2</i>	1.94	4.50	Receptor (TNFRSF)-interacting serine-threonine kinase 2
<i>RMND1</i>	-1.53	-1.42	Required for meiotic nuclear division 1 homolog
<i>RNF44</i>	1.73	1.18	Ring finger protein 44
<i>RPL29</i>	-2.19	-1.25	Ribosomal protein L29
<i>RPO1-1</i>	-1.64	-1.15	RNA polymerase 1-1
<i>RPP21</i>	-2.09	-1.33	Ribonuclease P 21 subunit
<i>RRP12</i>	1.47	1.50	Ribosomal RNA processing 12 homolog
<i>RSPH1</i>	-1.60	-1.52	Radial spoke head 1 homolog
<i>RXRB</i>	-2.37	-1.23	Retinoid X receptor beta
<i>SAA3</i>	23.85	43.08	Serum amyloid A 3
<i>SAS</i>	-1.19	-1.22	Sarcoma amplified sequence
<i>SAS</i>	1.56	1.41	Superoxide dismutase 2, mitochondrial
<i>SAV1</i>	2.12	1.43	Salvador homolog 1
<i>SCCPDH</i>	-1.72	-1.34	Saccharopine dehydrogenase
<i>SCGB1A1</i>	-1.49	-1.30	Secretoglobin, family 1A, member 1
<i>SEC14L2</i>	-2.37	-1.54	SEC14-like 2
<i>SELE</i>	5.17	2.95	Selectin, endothelial cell
<i>SEMA3F</i>	-1.28	-1.59	Sema domain, Ig, short basic domain, secreted 3 F
<i>SERGEF</i>	-1.52	-1.55	Secretion regulating guanine nucleotide exchange factor
<i>SERPINA3H</i>	3.71	5.04	Serine (or cysteine) peptidase inhibitor, clade A, member 3H

<i>SERTAD2</i>	1.22	1.40	SERTA domain containing 2
<i>SH3GLB2</i>	-1.37	-1.28	SH3-domain GRB2-like endophilin B2
<i>SHARPIN</i>	-2.92	-1.24	SHANK-associated RH domain interacting protein
<i>SIAH1B</i>	1.41	1.17	Seven in absentia 1B
<i>SKP2</i>	1.53	1.46	S-phase kinase-associated protein 2 (p45)
<i>SLC11A1</i>	-1.25	-1.26	Solute carrier family 11, member 1
<i>SLC24A6</i>	-1.48	-1.45	Solute carrier family 24, member 6
<i>SLC25A25</i>	2.56	2.26	Solute carrier family 25 , member 25
<i>SLC25A45</i>	-1.33	-1.43	Solute carrier family 25, member 45
<i>SLC2A6</i>	3.83	6.75	Solute carrier family 2 , member 6
<i>SLC41A3</i>	-1.39	-2.27	Solute carrier family 41, member 3
<i>SLC44A2</i>	-1.41	-1.38	Solute carrier family 44, member 2
<i>SLC44A4</i>	-1.69	-1.71	Solute carrier family 44, member 4
<i>SLC6A6</i>	1.26	1.22	Solute carrier family 6, member 6
<i>SLC7A11</i>	35.30	1.86	Solute carrier family 7, member 11
<i>SLC7A6</i>	1.89	1.41	Solute carrier family 7, member 6
<i>SLC9A3R2</i>	-1.27	-1.66	Solute carrier family 9, member 3 regulator 2
<i>SLCO2B1</i>	-1.63	-2.74	Solute carrier organic anion transporter family, member 2b1
<i>SLPI</i>	1.70	2.59	Secretory leukocyte peptidase inhibitor
<i>SMG6</i>	-1.31	-1.53	Smg-6 homolog, nonsense mediated mRNA decay factor
<i>SMPD2</i>	-1.31	-1.52	Sphingomyelin phosphodiesterase 2, neutral
<i>SNAPIN</i>	-1.17	-1.29	SNAP-associated protein
<i>SNX10</i>	1.61	1.75	Sorting nexin 10
<i>SNX18</i>	1.39	1.48	Sorting nexin 18
<i>SNX21</i>	-1.27	-1.59	Sorting nexin family member 21
<i>SOAT1</i>	-1.30	-1.35	Sterol O-acyltransferase 1
<i>SOCS2</i>	1.34	1.51	Suppressor of cytokine signaling 2
<i>SOCS3</i>	4.17	1.83	Suppressor of cytokine signaling 3
<i>SORD</i>	-1.54	-1.58	Sorbitol dehydrogenase
<i>SORT1</i>	-1.22	-1.41	Sortilin 1
<i>SOX13</i>	2.38	1.57	SRY-box containing gene 13
<i>SP5</i>	2.30	1.85	Trans-acting transcription factor 5
<i>SPAG5</i>	-1.53	-1.35	Sperm associated antigen 5
<i>SPHK1</i>	-1.56	-1.59	Sphingosine kinase 1
<i>SPON2</i>	-2.17	-2.16	Spondin 2, extracellular matrix protein
<i>SQLE</i>	1.44	1.50	Squalene epoxidase
<i>SQSTM1</i>	2.08	1.33	Sequestosome 1
<i>SRM</i>	1.53	1.55	Spermidine synthase
<i>ST3GAL1</i>	2.30	1.78	ST3 beta-galactoside alpha-2,3-sialyltransferase 1
<i>STAMBP</i>	-1.40	-1.40	Stam binding protein
<i>STAT1</i>	1.83	1.39	Signal transducer and activator of transcription 1

<i>STEAP2</i>	1.27	1.44	Six transmembrane epithelial antigen of prostate 2
<i>STK39</i>	-1.24	-1.18	Serine/threonine kinase 39, STE20/SPS1 homolog
<i>STX5A</i>	-1.14	-1.15	Syntaxin 5A
<i>STX6</i>	1.30	1.84	Syntaxin 6
<i>SUPT3H</i>	-1.98	-1.52	Suppressor of Ty 3 homolog
<i>SUPT4H1</i>	-1.25	-1.23	Suppressor of Ty 4 homolog 1
<i>TAF12</i>	-1.51	-1.18	TAF12 RNA polymerase II, TBP-associated factor
<i>TANK</i>	1.30	1.95	TRAF family member-associated Nf-kappa B activator
<i>TBC1D22A</i>	-1.11	-1.45	TBC1 domain family, member 22a
<i>TBC1D2B</i>	1.57	1.35	TBC1 domain family, member 2B
<i>TBCEL</i>	1.19	1.23	Tubulin folding cofactor E-like
<i>TBL1X</i>	1.56	1.35	Transducin (beta)-like 1 X-linked
<i>TCEA3</i>	-1.34	-2.14	Transcription elongation factor A 3
<i>TCP1</i>	1.30	1.26	T-complex protein 1
<i>TFRC</i>	1.30	1.35	Transferrin receptor
<i>TGM1</i>	1.82	1.81	Transglutaminase 1, K polypeptide
<i>THEM2</i>	-1.94	-1.39	Thioesterase superfamily member 2
<i>THNSL2</i>	-1.74	-2.27	Threonine synthase-like 2
<i>TIAL1</i>	1.59	1.68	Tia1 cytotoxic granule-associated RNA binding protein-like 1
<i>TIAM1</i>	1.30	1.61	T-cell lymphoma invasion and metastasis 1
<i>TLR2</i>	12.72	7.45	Toll-like receptor 2
<i>TMED8</i>	1.31	1.65	Transmembrane emp24 domain containing 8
<i>TMEM111</i>	-1.36	-1.08	Transmembrane protein 111
<i>TMEM132A</i>	-1.26	-1.23	Transmembrane protein 132A
<i>TMEM143</i>	-1.63	-2.05	Transmembrane protein 143
<i>TMEM167</i>	1.34	1.56	Transmembrane protein 167
<i>TMEM184A</i>	-1.72	-1.29	Transmembrane protein 184a
<i>TMEM23</i>	1.66	2.07	Sphingomyelin synthase 1
<i>TMEM32</i>	1.54	1.48	Transmembrane protein 32
<i>TMEM49</i>	1.53	1.51	Transmembrane protein 49
<i>TMEM53</i>	-2.07	-2.17	Transmembrane protein 53
<i>TMEM86A</i>	-1.34	-1.49	Transmembrane protein 86A
<i>TMEM93</i>	1.17	1.18	Transmembrane protein 93
<i>TNF</i>	51.06	9.06	Tumor necrosis factor
<i>TNFAIP2</i>	3.92	2.45	Tumor necrosis factor, alpha-induced protein 2
<i>TNFAIP3</i>	5.19	49.16	Tumor necrosis factor, alpha-induced protein 3
<i>TNFRSF11B</i>	1.64	4.41	Tumor necrosis factor receptor superfamily, member 11b
<i>TNIP1</i>	3.41	1.94	TNFAIP3 interacting protein 1
<i>TNRC6A</i>	1.68	1.14	Trinucleotide repeat containing 6a
<i>TOP1</i>	1.91	3.15	Topoisomerase I
<i>TPM1</i>	1.36	1.34	Tropomyosin 1, alpha

<i>TRAF3</i>	1.81	2.36	TNF receptor-associated factor 3
<i>TRAFD1</i>	-1.27	-1.46	TRAF type zinc finger domain containing 1
<i>TRAPPC1</i>	-1.39	-1.25	Trafficking protein particle complex 1
<i>TRAPPC6A</i>	-1.45	-1.40	Trafficking protein particle complex 6A
<i>TRIB2</i>	-1.25	-1.42	Tribbles homolog 2
<i>TRIM21</i>	2.25	1.37	Tripartite motif-containing 21
<i>TRIM32</i>	1.32	1.17	Tripartite motif-containing 32
<i>TRP53</i>	2.46	1.87	Transformation related protein 53
<i>TSC22D3</i>	-1.30	-1.41	TSC22 domain family 3
<i>TUFT1</i>	-1.34	-1.38	Tuftelin 1
<i>TUSC4</i>	-1.20	-1.32	Tumor suppressor candidate 4
<i>TWF2</i>	-1.28	-1.38	Twinfilin, actin-binding protein, homolog 2
<i>TXNDC15</i>	-1.30	-1.19	Thioredoxin domain containing 15
<i>TXNRD2</i>	-1.23	-1.29	Thioredoxin reductase 2
<i>TYK2</i>	1.52	1.33	Tyrosine kinase 2
<i>UAP1L1</i>	-1.47	-1.47	UDP-N-acetylglucosamine pyrophosphorylase 1-like 1
<i>UBAC1</i>	-1.28	-1.22	Ubiquitin associated domain containing 1
<i>UBE2D3</i>	1.31	1.54	Ubiquitin-conjugating enzyme E2D 3
<i>UBE2E2</i>	1.17	1.16	Ubiquitin-conjugating enzyme E2E 2
<i>UBE2Q2</i>	1.52	1.84	Ubiquitin-conjugating enzyme E2Q
<i>UBXD1</i>	-1.33	-1.28	UBX domain containing 1
<i>UCK2</i>	1.34	1.25	Uridine-cytidine kinase 2
<i>UPK1B</i>	-1.31	-1.18	Uroplakin 1B
<i>USE1</i>	-1.53	-1.26	Unconventional SNARE in the ER 1 homolog
<i>USO1</i>	-1.50	-1.19	USO1 homolog, vesicle docking protein
<i>USP20</i>	-1.52	-1.69	Ubiquitin specific peptidase 20
<i>USP39</i>	1.21	1.24	Ubiquitin specific peptidase 39
<i>USP6NL</i>	1.31	1.44	USP6 N-terminal like
<i>VCAM1</i>	2.87	8.35	Vascular cell adhesion molecule 1
<i>VEGFA</i>	1.18	1.62	Vascular endothelial growth factor A
<i>VEZF1</i>	1.18	1.21	Vascular endothelial zinc finger 1
<i>VPS16</i>	-1.20	-1.19	Vacuolar protein sorting 16
<i>VPS25</i>	-1.56	-1.30	Vacuolar protein sorting 25
<i>VRK3</i>	-1.61	-1.35	Vaccinia related kinase 3
<i>WDR21</i>	-1.32	-1.40	WD repeat domain 21
<i>WDR59</i>	-2.09	-1.41	WD repeat domain 59
<i>WFDC2</i>	-1.35	-1.21	WAP four-disulfide core domain 2
<i>WFDC3</i>	-1.51	-1.61	WAP four-disulfide core domain 3
<i>YIPF3</i>	-1.21	-1.21	Yip1 domain family, member 3
<i>YOD1</i>	1.30	1.60	YOD1 OTU deubiquitinating enzyme 1 homologue
<i>YPEL3</i>	-1.27	-1.57	Yippee-like 3

<i>ZC3H12A</i>	4.47	10.14	Zinc finger CCCH type containing 12A
<i>ZDHHC13</i>	1.38	1.39	Zinc finger, DHHC domain containing 13
<i>ZER1</i>	-1.53	-1.65	Zer-1 homolog
<i>ZFHX3</i>	1.75	1.11	Zinc finger homeobox 3
<i>ZFP131</i>	1.30	1.26	Zinc finger protein 131
<i>ZFP160</i>	1.97	1.50	Zinc finger protein 160
<i>ZFP238</i>	1.13	1.55	Zinc finger protein 238
<i>ZFP365</i>	1.40	1.46	Zinc finger protein 365
<i>ZFP36L1</i>	1.18	1.20	Zinc finger protein 36, C3H type-like 1
<i>ZFP57</i>	1.81	2.74	Zinc finger protein 57
<i>ZFP770</i>	1.90	1.69	Zinc finger protein 770
<i>ZFR</i>	1.93	1.85	Zinc finger RNA binding protein
<i>ZHX2</i>	2.40	2.82	Zinc fingers and homeoboxes 2
<i>ZMYM3</i>	-2.07	-1.49	Zinc finger, MYM-type 3
<i>ZRANB3</i>	-1.56	-1.66	Zinc finger, RAN-binding domain containing 3
<i>ZRSR2</i>	1.43	1.27	Zinc finger (CCCH type), RNA binding motif and serine/arginine rich 2 (Zrsr2)

Supplemental Table 2. Time course of pathogen burden. Mice were treated by aerosol with PBS (sham) or Pam2-ODN 24 h prior to infection with *P. aeruginosa*. The lungs, spleens and livers of infected mice were harvested under sterile conditions at designated time points, homogenized in 1 ml sterile PBS, and submitted to serial dilution culture. Reported are CFU/ml. All PBS-treated mice died prior to the 48 h harvest. (n = 3-6 mice/condition)

	Treatment	0 h		24 h		48 h	
		<u>Mean</u>	<u>SEM</u>	<u>Mean</u>	<u>SEM</u>	<u>Mean</u>	<u>SEM</u>
LUNGS	PBS	3 x10 ⁶	1 x10 ⁵	6 x10 ⁶	3 x10 ⁵	All Dead	-
	Pam2-ODN	5 x10 ⁵	6 x10 ⁴	5 x10 ³	2 x10 ³	0	-
SPLEEN	PBS	0	-	6 x10 ⁴	2 x10 ³	All Dead	-
	Pam2-ODN	0	-	0	-	0	-
LIVER	PBS	0	-	6 x10 ⁴	3 x10 ³	All Dead	-
	Pam2-ODN	0	-	0	-	0	-